# Chapter 11

# Mechanical Properties: Fast Fracture

*The careful text-books measure*
*(Let all who build beware!)*
*The load, the shock, the pressure*
*Material can bear.*
*So when the buckled girder*
*Lets down the grinding span.*
*The blame of loss, or murder,*
*Is laid upon the man.*
*Not on the stuff — the Man!*

R. Kipling, "*Hymn of the Breaking Strain*"

## 11.1 Introduction

Sometime before the dawn of civilization, some hominid discovered that the edge of a broken stone was quite useful for killing prey and warding off predators. This seminal juncture in human history has been recognized by archeologists who refer to it as the stone age. C. Smith[178] goes further by stating, "Man probably owes his very existence to a basic property of inorganic matter, the brittleness of certain ionic compounds." In this context, Kipling's hymn and J. E. Gordon's statement[179] that "The worst sin in an engineering material is not lack of strength or lack of stiffness, desirable as these properties are, but lack of toughness, that is to say, lack of resistance to the propagation of cracks" stand in sharp contrast. But it is this contrast that in a very real sense summarizes the short history of technical ceramics: what was good enough for millennia now falls short. After all, the consequences of a broken mirror are not as dire as those of, say, an exploding turbine blade. It could be argued, with some justification, that were it not for their brittleness, the use of ceramics for structural applications, especially

[178] C. S. Smith, *Science*, **148**:908 (1965).
[179] J. E. Gordon, *The New Science of Engineering Materials*, 2d ed., Princeton University Press, Princeton, New Jersey, 1976.

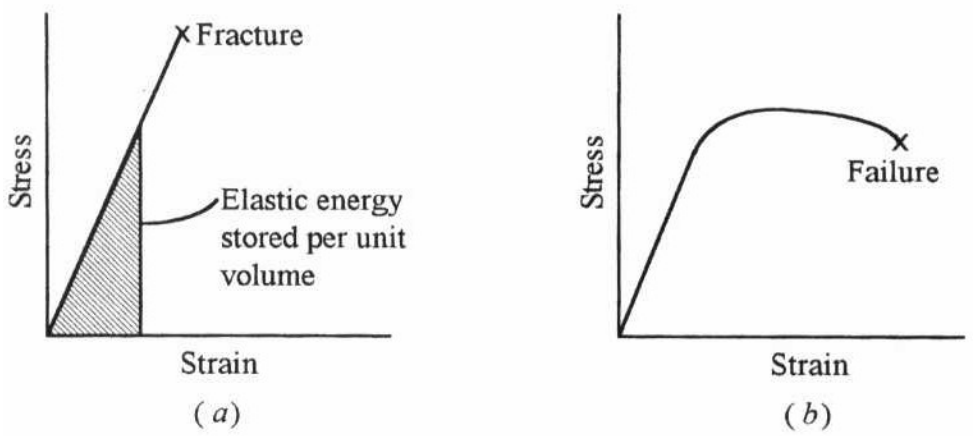


**Figure 11.1** Typical stress–strain curves for (*a*) brittle solids and (*b*) ductile materials.

at elevated temperatures, would be much more widespread since they possess other very attractive properties such as hardness, stiffness, and oxidation and creep resistance.

As should be familiar to most, the application of a stress to any solid will initially result in a reversible elastic strain that is followed by either fracture without much plastic deformation (Fig. 11.1*a*) or fracture that is preceded by plastic deformation (Fig. 11.1*b*). Ceramics and glasses fall in the former category and are thus considered brittle solids, whereas most metals and polymers above their glass transition temperature fall into the latter category.

The theoretical stress level at which a material is expected to fracture by bond rupture was discussed in Chap. 4 and estimated to be on the order of $Y/10$, where $Y$ is Young's modulus. Given that $Y$ for ceramics (see Table 11.1) ranges between 100 and 500 GPa, the expected "ideal" fracture stress is quite high — on the order of 10 to 50 GPa. For reasons that will become apparent shortly, the presence of flaws, such as shown in Fig. 11.2, in brittle solids will greatly reduce the stress at which they fail. Conversely, it is well established that extraordinary strengths can be achieved if they are flaw-free. For example, a defect-free silica glass rod can be elastically deformed to stresses that exceed 5 GPa! Thus it may be concluded, correctly one might add, that certain flaws within a material serve to promote fracture at stress levels that are well below the ideal fracture stress.

The stochastic nature of flaws present in brittle solids together with the flaw sensitivity of the latter has important design ramifications as well. Strength variations of ±25 percent from the mean are not uncommon and are quite large when compared to, say, the spread of flow stresses in metals, which are typically within just a few percent. Needless to say, such variability, together with the sudden nature of brittle failure, poses a veritable challenge for design engineers considering using ceramics for structural and other critical applications.

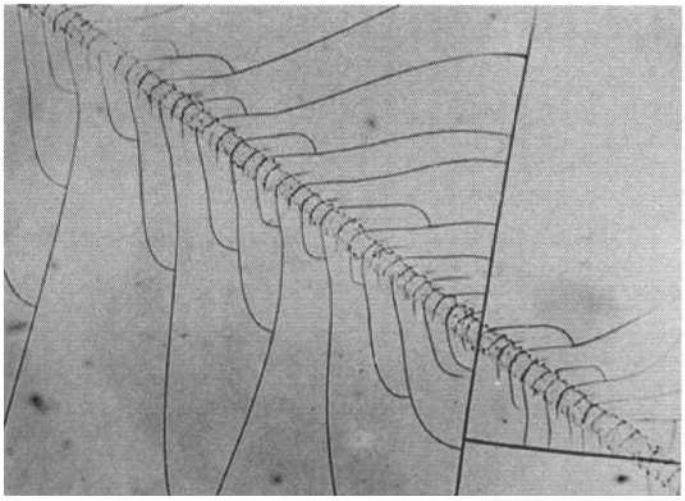

**Figure 11.2** Surface cracks caused by the accidental contact of a glass surface with dust particles or another solid surface can result in significant reductions in strength.

Flaws, their shape, and their propagation are the central themes of this chapter. The various aspects of brittle failure are discussed from several viewpoints. The concepts of fracture toughness and flaw sensitivity are discussed first. The factors influencing the strengths of ceramics are dealt with in Sec. 11.3.[180] Toughening mechanisms are dealt with in Sec. 11.4. Section 11.5 introduces the statistics of brittle failure and a methodology for design.

## 11.2 Fracture Toughness

### 11.2.1 Flaw Sensitivity

To illustrate what is meant by flaw or notch sensitivity, consider the schematic of what occurs at the base of an atomically sharp crack upon the application of a load $F_{app}$. For a crack-free sample (Fig. 11.3*a*), each chain of atoms will carry its share of the load $F/n$, where $n$ is the number of chains, i.e., the applied stress $\sigma_{app}$ is said to be uniformly distributed. The introduction of a surface crack results in a stress redistribution such that the load that was supported by the severed bonds is now being carried by only a few bonds at the crack tip (Fig. 11.3*b*). Said otherwise, the presence of a flaw will *locally amplify the applied stress at the crack tip* $\sigma_{tip}$. As $\sigma_{app}$ is increased, $\sigma_{tip}$ increases accordingly and moves up the stress versus interatomic distance curve, as shown in Fig. 11.3*c*. As long as $\sigma_{tip} < \sigma_{max}$, the situation is stable and the flaw will not propagate. However, if at any time $\sigma_{tip}$ exceeds $\sigma_{max}$, the situation becomes catastrophically unstable (not

[180] The time-dependent mechanical properties such as creep and subcritical crack growth are dealt with separately in the next chapter.

unlike the bursting of a dam). Based on this simple picture, the reason why brittle fracture occurs rapidly and without warning, with cracks propagating at velocities approaching the speed of sound, should now be obvious. Furthermore, it should also be obvious why ceramics are much stronger in compression than in tension.

To be a little more quantitative in predicting the applied stress that would lead to failure, $\sigma_{tip}$ would have to be calculated and equated to $\sigma_{max}$

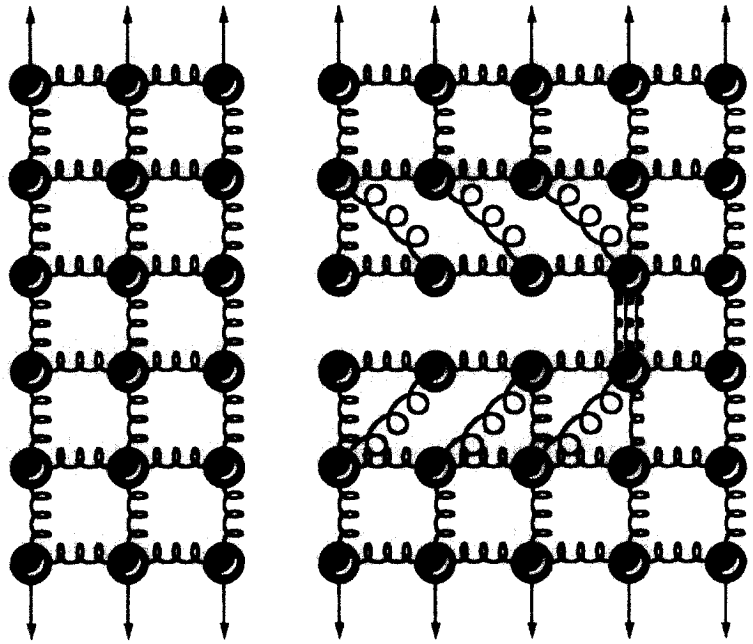

(*a*) (*b*)

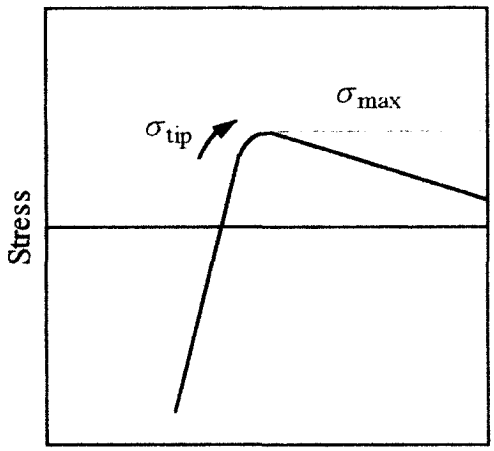


(*c*)

**Figure 11.3** (*a*) Depiction of a uniform stress. (*b*) Stress redistribution as a result of the presence of a crack. (*c*) For a given applied load, as the crack grows and the bonds are sequentially ruptured, $\sigma_{tip}$ moves up the stress versus displacement curve toward $\sigma_{max}$. When $\sigma_{tip} \approx \sigma_{max}$, catastrophic failure occurs. Note that this figure is identical to Fig. 4.6, except that here the $y$ axis represents the stress on the bond rather than the applied force.

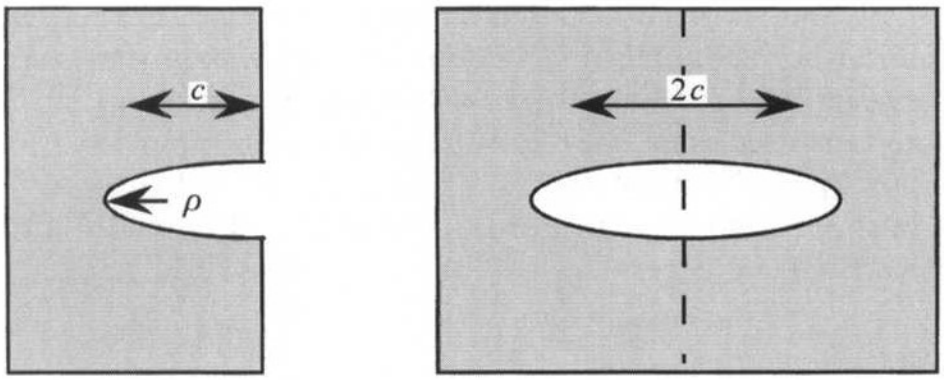


**Figure 11.4** (*a*) Surface crack of length $c$ and radius of curvature $\rho$. (*b*) Interior crack of length $2c$. Note that from a fracture point of view, they are equivalent.

or $Y/10$. Calculating $\sigma_{tip}$ is rather complicated (only the final result is given here) and is a function of the type of loading, sample, crack geometry, etc.[181] However, for a thin sheet, it can be shown that $\sigma_{tip}$ is related to the applied stress by

$$\sigma_{tip} = 2\sigma_{app}\sqrt{\frac{c}{\rho}} \tag{11.1}$$

where $c$ and $\rho$ are, respectively, the crack length and its radius of curvature[182] (Fig. 11.4).

Since, as noted above, fracture can be reasonably assumed to occur when $\sigma_{tip} = \sigma_{max} \approx Y/10$, it follows that

$$\sigma_f \approx \frac{Y}{20}\sqrt{\frac{\rho}{c}} \tag{11.2}$$

where $\sigma_f$ is the stress at fracture. This equation predicts that (1) $\sigma_f$ is inversely proportional to the square root of the flaw size and (2) sharp cracks, i.e., those with a small $\rho$, are more deleterious than blunt cracks. Both predictions are in good agreement with numerous experimental observations.

### 11.2.2 Energy Criteria for Fracture — The Griffith Criterion

An alternate and ultimately more versatile approach to the problem of fracture was developed in the early 1920s by Griffith.[183] His basic idea was

[181] C. E. Inglis, *Trans. Inst. Naval Archit.*, **55**:219 (1913).

[182] This equation strictly applies to a surface crack of length $c$, or an interior crack of length $2c$ in a thin sheet. Since the surface of the material cannot support a stress normal to it, this condition corresponds to the plane stress condition (the stress is two-dimensional). In thick components, the situation is more complicated, but for brittle materials the two expressions vary slightly.

[183] A. A. Griffith, *Phil. Trans. R. Acad.*, **A221**:163 (1920).

to balance the energy consumed in forming new surface as a crack propagates against the elastic energy released. The critical condition for fracture, then, occurs when the rate at which energy is released is greater than the rate at which it is consumed. The approach taken here is a simplified version of the original approach, and it entails deriving an expression for the energy changes resulting from the introduction of a flaw of length $c$ in a material subjected to a uniform stress $\sigma_{app}$.

**Strain energy**

When a solid is uniformly elastically stressed, all bonds in the material elongate and the work done by the applied stress is converted to elastic energy that is stored in the stretched bonds. The magnitude of the elastic energy stored per unit volume is given by the area under the stress-strain curve[184] (Fig. 11.1*a*), or

$$U_{elas} = \frac{1}{2}\varepsilon\sigma_{app} = \frac{1}{2}\frac{\sigma_{app}^2}{Y} \tag{11.3}$$

The total energy of the parallelopiped of volume $V_0$ subjected to a uniform stress $\sigma_{app}$ (Fig. 11.5*a*) increases to

$$U = U_0 + V_0 U_{elas} = U_0 + \frac{V_0\sigma_{app}^2}{2Y} \tag{11.4}$$

where $U_0$ its free energy in the absence of stress.

In the presence of a surface crack of length $c$ (Fig. 11.5*b*), it is fair to assume that some volume around that crack will relax (i.e., the bonds in that volume will relax and lose their strain energy). Assuming — it is not a bad assumption, as will become clear shortly — that the relaxed volume is given by the shaded area in Fig. 11.5*b*, it follows that the strain energy of the system in the presence of the crack is given by

$$U_{strain} = U_0 + \frac{V_0\sigma_{app}^2}{2Y} - \frac{\sigma_{app}^2}{2Y}\left[\frac{\pi c^2 t}{2}\right] \tag{11.5}$$

where $t$ is the thickness of the plate. The third term represents the *strain energy released* in the relaxed volume.

[184] When a bond is stretched, energy is stored in that bond in the form of elastic energy. This energy can be converted to other forms of energy as any schoolboy with a slingshot can attest; the elastic energy stored in the rubber band is converted into kinetic energy of the projectile. If by chance a pane of glass comes in the way of the projectile, that kinetic energy will in turn be converted to other forms of energy such as thermal, acoustic, and surface energy. In other words, the glass will shatter and some of the kinetic energy will have created new surfaces.

**Surface energy**

To form a crack of length $c$, an energy expenditure of

$$U_{surf} = 2\gamma ct \tag{11.6}$$

is required, where $\gamma$ is the intrinsic surface energy of the material. The factor 2 arises because two (bottom and top) new surfaces are created by the fracture event.

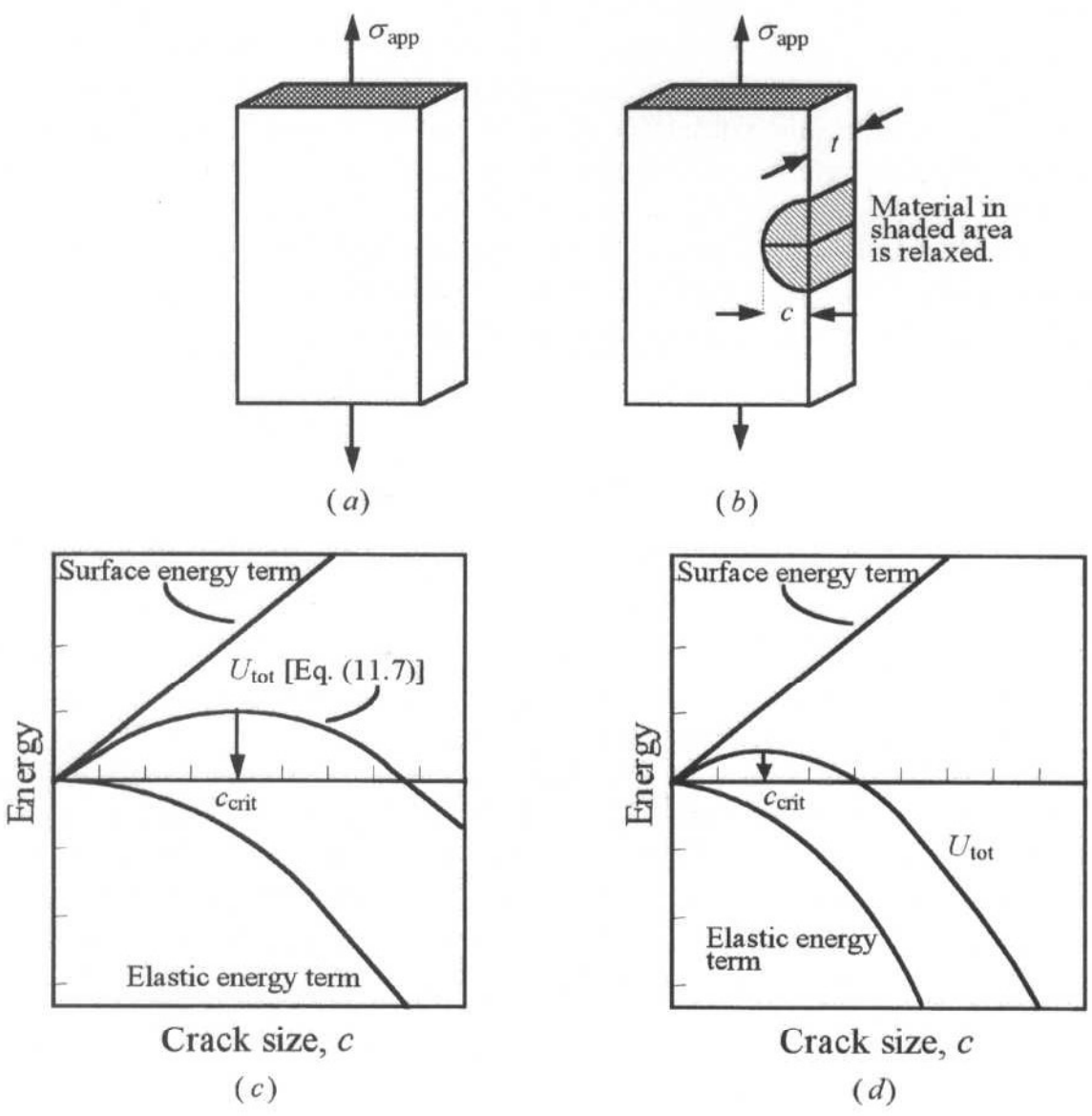


**Figure 11.5** (*a*) Uniformly stressed solid. (*b*) Relaxed volume in vicinity of crack of length $c$. (*c*) Plot of Eq. (11.7) as a function of $c$. The top curve represents the surface energy term, and the lower curve represents the strain energy release term. Curve labeled $U_{tot}$ is sum of the two curves. The critical crack length $c_{crit}$ at which fast fracture will occur corresponds to the maximum. (*d*) Plot of Eq. (11.7) on the same scale as in part (*c*) but for $\sqrt{2}$ times the applied stress applied in (*c*). Increasing the applied stress by that factor reduces $c_{crit}$ by a factor of 2.

The total energy change of the system upon introduction of the crack is simply the sum of Eqs. (11.5) and (11.6), or

$$U_{\text{tot}} = U_0 + \frac{V_0\sigma_{\text{app}}^2}{2Y} - \frac{\sigma_{\text{app}}^2}{2Y}\left[\frac{\pi c^2 t}{2}\right] + 2\gamma ct \tag{11.7}$$

Since the surface energy term scales with $c$ and the strain energy term scales with $c^2$, $U_{\text{tot}}$ has to go through a *maximum* at a certain critical crack size $c_{\text{crit}}$ (Fig. 11.5*c*). This is an important result since it implies that extending a crack that is smaller than $c_{\text{crit}}$ *consumes rather than liberates energy and is thus stable.* In contrast, *flaws that are longer than* $c_{\text{crit}}$ *are unstable since extending them releases more energy than is consumed.* Note that increasing the applied stress (Fig. 11.5*d*) will result in failure at smaller critical flaw sizes. For instance, a solid for which the size of the largest[185] flaw lies somewhere between those shown in Fig. 11.5*c* and *d* will *not* fail at the stress shown in Fig. 11.5*c*, but will fail if that stress is increased (Fig. 11.5*d*).

The location of the maximum is determined by differentiating Eq. (11.7) and equating it to zero. Carrying out the differentiation, replacing $\sigma_{\text{app}}$ by $\sigma_f$, and rearranging terms, one can show that the condition for failure is

$$\sigma_f\sqrt{\pi c_{\text{crit}}} = 2\sqrt{\gamma Y} \tag{11.8}$$

A more exact calculation yields

$$\boxed{\sigma_f\sqrt{\pi c_{\text{crit}}} \geq \sqrt{2\gamma Y}} \tag{11.9}$$

and is the expression used in subsequent discussions.[186] This equation predicts that a critical combination of *applied stress and flaw size is required to cause failure.* The combination $\sigma\sqrt{\pi c}$ occurs so often in discussing fast fracture that it is abbreviated to a single symbol $K_{\text{I}}$ with units $\text{MPa}\cdot\text{m}^{1/2}$, and is referred to as the **stress intensity factor**. Similarly, the combination of terms on the right-hand side of Eq. (11.9), sometimes referred to as the **critical stress intensity factor**, or more commonly the **fracture toughness**, is abbreviated by the symbol $K_{\text{Ic}}$. Given these abbreviations, the condition for fracture can be succinctly rewritten as

$$\boxed{K_{\text{I}} \geq K_{\text{Ic}}} \tag{11.10}$$

Equations (11.9) and (11.10) were derived with the implicit assumption that the only factor keeping the crack from extending was the creation of new

[185] The largest flaw is typically the one that will cause failure, since it becomes critical before other smaller flaws (see Fig. 11.8*a*).

[186] Comparing Eqs. (11.8) and (11.9) shows that the estimate of the volume over which the stress is relieved in Fig. 11.5*b* was off by a factor of $\sqrt{2}$, which is not too bad.

**Table 11.1** Data for Young's modulus $Y$, Poisson's ratio, and $K_{Ic}$ values of selected ceramics at ambient temperatures[†]

| | $Y$, (GPa) | Poisson's ratio | $K_{Ic}$, MPa · $m^{1/2}$ | Vickers hardness, GPa |
|---|---|---|---|---|
| **Oxides** | | | | |
| $Al_2O_3$ | 390 | 0.20–0.25 | 2.0–6.0 | 19.0–26.0 |
| $Al_2O_3$ (single crystal, $10\bar{1}2$) | 340 | | 2.2 | |
| $Al_2O_3$ (single crystal, 0001) | 460 | | >6.0 | |
| $BaTiO_3$ | 125 | | | |
| BeO | 386 | 0.34 | | 0.8–1.2 |
| $HfO_2$ (monoclinic) | 240 | | | |
| MgO | 250–300 | 0.18 | 2.5 | 6.0–10.0 |
| $MgTi_2O_5$ | 250 | | | |
| $MgAl_2O_4$ | 248–270 | | 1.9–2.4 | 14.0–18.0 |
| Mullite [fully dense] | 230 | 0.24 | 2.0–4.0 | 15.0 |
| $Nb_2O_5$ | 180 | | | |
| $PbTiO_3$ | 81 | | | |
| $SiO_2$ (quartz) | 94 | 0.17 | | 12.0 (011) |
| $SnO_2$ | 263 | 0.29 | | |
| $TiO_2$ | 282–300 | | | 10.0 ± 1.0 |
| $ThO_2$ | 250 | | 1.6 | 10.0 |
| $Y_2O_3$ | 175 | | 1.5 | 7.0–9.0 |
| $Y_3Al_5O_{12}$ | | | | 18.0 ± 1.0 |
| ZnO | 124 | | | 2.3 ± 1.0 |
| $ZrSiO_4$ (zircon) | 195 | 0.25 | | ≈15.0 |
| $ZrO_2$ (cubic) | 220 | 0.31 | 3.0–3.6 | 12.0–15.0 |
| $ZrO_2$ (partially stabilized) | 190 | 0.30 | 3.0–15.0 | 13.0 |
| **Carbides, Borides, and Nitrides and Silicides** | | | | |
| AlN | 308 | 0.25 | | 12.0 |
| $B_4C$ | 417–450 | 0.17 | | 30.0–38.0 |
| BN | 675 | | | |
| Diamond | 1000 | | | |
| $MoSi_2$ | 400 | | | |
| Si | 107 | 0.27 | | 10.0 |
| SiC [hot pressed] | 440 ± 10 | 0.19 | 3.0–6.0 | 26.0–36.0 |
| SiC (single crystal) | 460 | | 3.7 | |
| $Si_3N_4$ Hot Pressed (dense) | 300–330 | 0.22 | 3.0–10.0 | 17.0–30.0 |
| $TiB_2$ | 500–570 | 0.11 | | 18.0–34.0 |
| TiC | 456 | 0.18 | 3.0–5.0 | 16.0–28.0 |
| WC | 450–650 | | 6.0–20.0 | |
| $ZrB_2$ | 440 | 0.14 | | 22.0 |
| **Halides and Sulfides** | | | | |
| $CaF_2$ | 110 | | 0.80 | 1.800 |
| KCl (forged single crystal) | 24 | | ≈0.35 | 0.120 |

**Table 11.1** *Continued*

| | $Y$, (GPa) | Poisson's ratio | $K_{Ic}$, MPa · $m^{1/2}$ | Vickers hardness, GPa |
|---|---|---|---|---|
| $MgF_2$ | 138 | | 1.00 | 6.000 |
| $SrF_2$ | 88 | | 1.00 | 1.400 |
| **Glasses and Glass Ceramics** | | | | |
| Aluminosilicate (Corning 1720) | 89 | 0.24 | 0.96 | 6.6 |
| Borosilicate (Corning 7740) | 63 | 0.20 | 0.75 | 6.5 |
| Borosilicate (Corning 7052) | 57 | 0.22 | | |
| LAS (glass-ceramic) | 100 | 0.30 | 2.00 | |
| Silica (fused) | 72 | 0.16 | 0.80 | 6.0–9.0 |
| Silica (96%) | 66 | | 0.70 | |
| Soda Lime Silica Glass | 69 | 0.25 | 0.82 | 5.5 |

† The fracture toughness is a function of microstructure. The values given here are mostly for comparison's sake.

surface. This is only true, however, for extremely brittle systems such as inorganic glasses. In general, however, when other energy dissipating mechanisms, such a plastic deformation at the crack tip, are operative, $K_{Ic}$ is defined as

$$\boxed{K_{Ic} = \sqrt{YG_c}} \tag{11.11}$$

where $G_c$ is the **toughness** of the material in joules per square meter. For purely brittle solids,[187] the toughness approaches the limit $G_c = 2\gamma$. Table 11.1 lists Young's modulus, Poisson's ratio, and $K_{Ic}$ values of a number of ceramic materials. It should be pointed out that since (see below) $K_{Ic}$ is a material property that is also microstructure-dependent, the values listed in Table 11.1 are to be used with care.

Finally it is worth noting that the Griffith approach, Eq. (11.10), can be reconciled with Eq. (11.2) by assuming that $\rho$ is on the order of $10r_0$, where $r_0$ is the equilibrium interionic distance (see Prob. 11.3). In other words, the Griffith approach implicitly assumes that the flaws are atomically sharp, a fact that must be borne in mind when one is experimentally determining $K_{Ic}$ for a material.

To summarize: fast fracture will occur in a material when the product of the applied stress and the square root of the flaw dimension are comparable to that material's fracture toughness.

[187] Under these conditions, one may calculate the surface energy of a solid from a measurement of $K_{Ic}$ (see the section on measuring surface energies in Chap. 4).

**WORKED EXAMPLE 11.1**

(*a*) A sharp edge notch 120 μm deep is introduced in a thin magnesia plate. The plate is then loaded in tension normal to the plane of the notch. If the applied stress is 150 MPa, will the plate survive? (*b*) Would your answer change if the notch were the same length but was as internal notch (Fig. 11.4*b*) instead of an edge notch?

**Answer**

(*a*) To determine whether the plate will survive the applied stress, the stress intensity at the crack tip needs to be calculated and compared to the fracture toughness of MgO, which according to Table 11.1 is 2.5 MPa · $m^{1/2}$.

$K_I$ in this case is given

$$K_I = \sigma\sqrt{\pi c} = 150\sqrt{3.14 \times 120 \times 10^{-6}} = 2.91 \text{ MPa} \cdot \text{m}^{1/2}$$

Since this value is greater than $K_{Ic}$ for MgO, it follows that the plate will fail.

(*b*) In this case, because the notch is an internal one, it is not as detrimental as a surface or edge notch and

$$K_I = \sigma\sqrt{\pi \frac{c}{2}} = 150\sqrt{3.14 \times 60 \times 10^{-6}} = 2.06 \text{ MPa} \cdot \text{m}^{1/2}$$

Since this value is <2.5 MPa · $m^{1/2}$ it follows that the plate would survive the applied load.

Before one explores the various strategies to increase the fracture toughness of ceramics, it is important to appreciate how $K_{Ic}$ is measured.

## Experimental Details: Measuring $K_{Ic}$

There are several techniques by which $K_{Ic}$ can be measured. The two most common methods entail measuring the fracture stress for a given geometry and known initial crack length and measuring the lengths of cracks emanating from hardness indentations.

### Fracture Stress

Equation (11.9) can be recast in its most general form

$$\Psi\sigma_{\text{frac}}\sqrt{\pi c} \geq K_{Ic} \tag{11.12}$$

where $\Psi$ is a dimensionless constant on the order of unity that depends on the sample shape, the crack geometry, and its relative size to the sample dimensions. This relationship suggests that to measure $K_{Ic}$, one would start with an *atomically* sharp crack [an implicit assumption made in deriving Eq. (11.10) — see Prob. 11.3] of length $c$ and measure the stress at which fracture occurs. Given

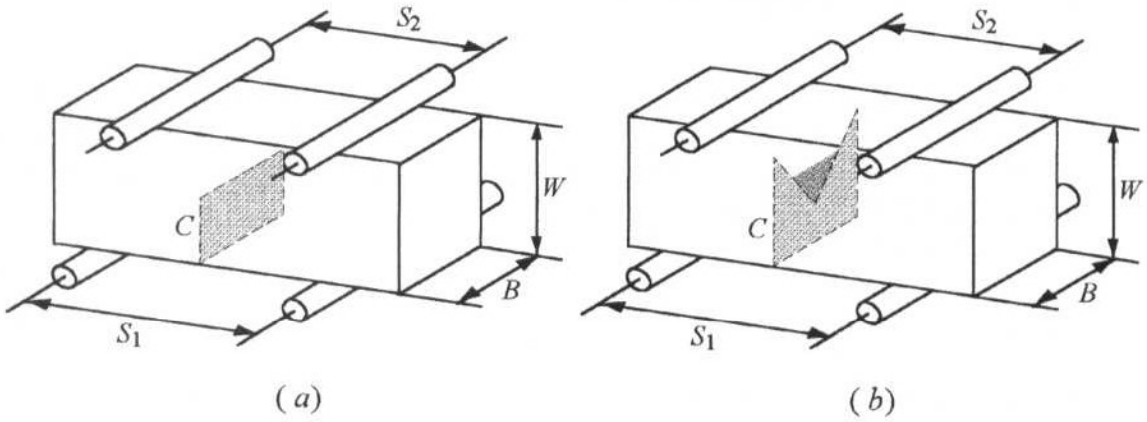


**Figure 11.6** (*a*) Schematic of single-edge notched beam specimen; (*b*) Chevron notch specimen.

the sample and crack geometries, $\Psi$ can be looked up in various fracture mechanics handbooks, and then $K_{Ic}$ is calculated from Eq. (11.12). Thus, in principle, it would appear that measuring $K_{Ic}$ is fairly straightforward; experimentally, however, the difficulty lies in introducing an atomically sharp crack.

Two of the more common test configurations are shown in Fig. 11.6. A third geometry not shown here is the **double torsion test**, which in addition to measuring $K_{Ic}$ can be used to measure crack velocity versus $K$ curves. This test is described in greater detail in the next chapter.

### Single-edge notched beam (SENB) test

In this test a notch of initial depth $c$ is introduced, usually by using a diamond wheel, on the tensile side of a flexure specimen (Fig. 11.6*a*). The sample is loaded until failure, and $c$ is taken as the initial crack length. Fracture toughness $K_{Ic}$ is calculated from

$$K_{Ic} = \frac{3\sqrt{c}(S_1 - S_2)\xi F_{fail}}{2BW^2}$$

where $F_{fail}$ is the load at which the specimen failed and $\xi$ is a calibration factor. The other symbols are defined in Fig. 11.6*a*. The advantage of this test lies in its simplicity — its major drawback, however, is that the condition that the crack be atomically sharp is, more often than not, unfulfilled, which causes one to overestimate $K_{Ic}$.

### Chevron notch (CN) specimen[188]

In this configuration, shown schematically in Fig. 11.6*b*, the chevron notch specimen looks quite similar to the SENB except for the vital difference that the shape of the initial crack is not flat but chevron-shaped, as shown by the shaded area. The constant widening of the crack front as it advances causes

[188] A *chevron* is a figure or a pattern having the shape of a V.

crack growth to be stable *prior* to failure. Since an increased load is required to continue crack extension, it is possible to create an atomically sharp crack in the specimen *before* final failure, which eliminates the need to precrack the specimen. The fracture toughness[189] is then related to the maximum load at fracture $F_{\text{fail}}$ and the minimum of a compliance function $\xi^*$.

$$K_{Ic} = \frac{(S_1 - S_2)\xi^* F_{\text{fail}}}{BW^{3/2}}$$

### General remarks

Unless care is taken in carrying out the fracture toughness measurements, different tests will result in different values of $K_{Ic}$. There are three reasons for this: (1) The sample dimensions were too small, compared to the process zone (which is the zone ahead of the crack tip that is damaged). (2) The internal stresses generated during machining of the specimens were not sufficiently relaxed before the measurements were made. (3) The crack tip was not atomically sharp. As noted above, if the fracture initiating the flaw is not atomically sharp, apparently higher $K_{Ic}$ values will be obtained. Thus although simple in principle, the measurement of $K_{Ic}$ is fraught with pitfalls, and care must be taken if reliable and accurate data are to be obtained.

### Hardness Indentation Method

Due to its simplicity, its nondestructive nature, and the fact that minimal machining is required to prepare the sample, the use of the Vickers hardness indentations to measure $K_{Ic}$ has become quite popular. In this method, a diamond indenter is applied to the surface of the specimen to be tested. Upon removal, the sizes of the cracks that emanate (sometimes) from the edges of the indent are measured, and the Vickers hardness $H$ in GPa of the material is calculated. A number of empirical and semiempirical relationships have been proposed relating $K_{Ic}$, $c$, $Y$, and $H$, and in general the expressions take the form

$$K_{Ic} = \Phi\sqrt{a}H\left(\frac{Y}{H}\right)^{0.4} f\left(\frac{c}{a}\right) \tag{11.13}$$

where $\Phi$ is a geometric constraint factor and $c$ and $a$ are defined in Fig. 11.7. The exact form of the expression used depends on the type of crack that emanates from the indent.[190] A cross-sectional view and a top view of the

[189] For more information, see J. Sung and P. Nicholson, *J. Amer. Cer. Soc.*, **72** (6):1033–1036 (1989).

[190] For more information, see G. R. Anstis, P. Chantikul, B. R. Lawn, and D. B. Marshall, *J. Amer. Cer. Soc.*, **64**:533 (1981), and R. Matsumoto, *J. Amer. Cer. Soc.*, **70**(C):366 (1987). See also Problem 11.9.

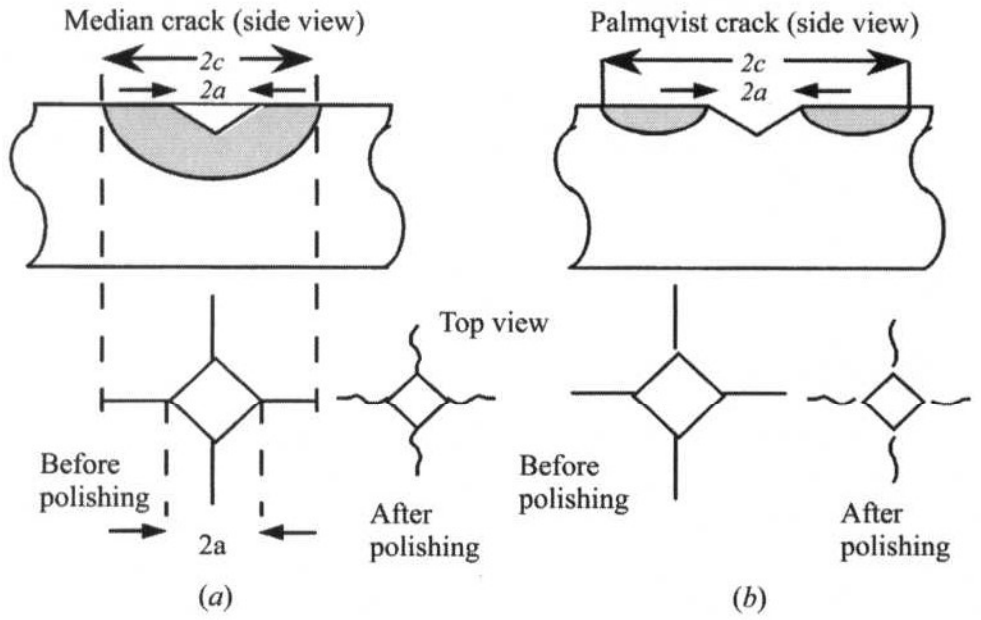


**Figure 11.7** Crack systems developed from the Vickers indents. (*a*) Side and top views of a median crack. (*b*) Top and side views of a Palmqvist crack.

two most common types of cracks of interest are shown in Fig. 11.7. At low loads, Palmqvist cracks are favored, while at high loads fully developed median cracks result. A simple way to differentiate between the two types is to polish the surface layers away; the median crack system will always remain connected to the inverted pyramid of the indent while the Palmqvist will become detached, as shown in Fig. 11.7*b*.

It should be emphasized that the $K_{Ic}$ values measured using this technique are usually not as precise as those from other more macroscopic tests.

### 11.2.3 Compressive and Other Failure Modes

Whereas it is now well established that tensile brittle failure usually propagates unstably when the stress intensity at the crack tip exceeds a critical value, the mechanics of compressive brittle fracture are more complex and not as well understood. Cracks in compression tend to propagate stably and twist out of their original orientation to propagate parallel to the compression axis, as shown in Fig. 11.8*b*. Fracture in this case is caused not by the unstable propagation of a single crack, as would be the case in tension (Fig. 11.8*a*), but by the slow extension and linking up of many cracks to form a crushed zone. Hence it is not the size of the largest crack that counts, but the size of the average crack $c_{av}$. The compressive stress to failure is still given by

$$\sigma_{fail} \approx Z \frac{K_{Ic}}{\sqrt{\pi c_{av}}} \tag{11.14}$$

but now $Z$ is a constant on the order of 15.

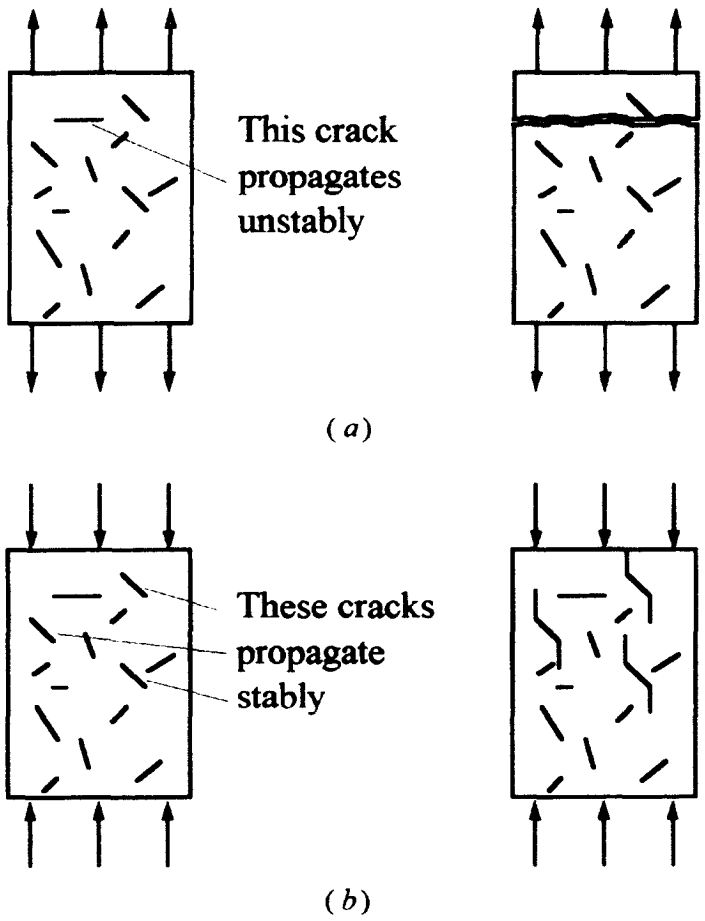


**Figure 11.8** (*a*) Fracture in ceramics due to preexisting flaws tested in tension. Failure occurs by the unstable propagation of the worst crack that is also most favorably oriented. (*b*) During compressive loading, many cracks propagate stably, eventually linking up and creating a crush zone.[191]

Finally, in general there are three modes of failure, known as modes I, II, and III. Mode I (Fig. 11.9*a*) is the one that we have been dealing with so far. Modes II and III are shown in Fig. 11.9*b* and *c*, respectively. The same energy concepts that apply to mode I also apply to modes II and III. Mode I, however, is by far the more pertinent to crack propagation in brittle solids.

### 11.2.4 Atomistic Aspects of Fracture

Up to this point, the discussion has been mostly couched in macroscopic terms. Flaws were shown to concentrate the applied stress at their tip which ultimately led to failure. No distinction was made between brittle and ductile materials, and yet experience clearly indicates that the different classes of materials behave quite differently — after all, the consequences

[191] Adapted from M. F. Ashby and D. R. Jones, *Engineering Materials*, vol. 2, Pergamon Press, New York, 1986.

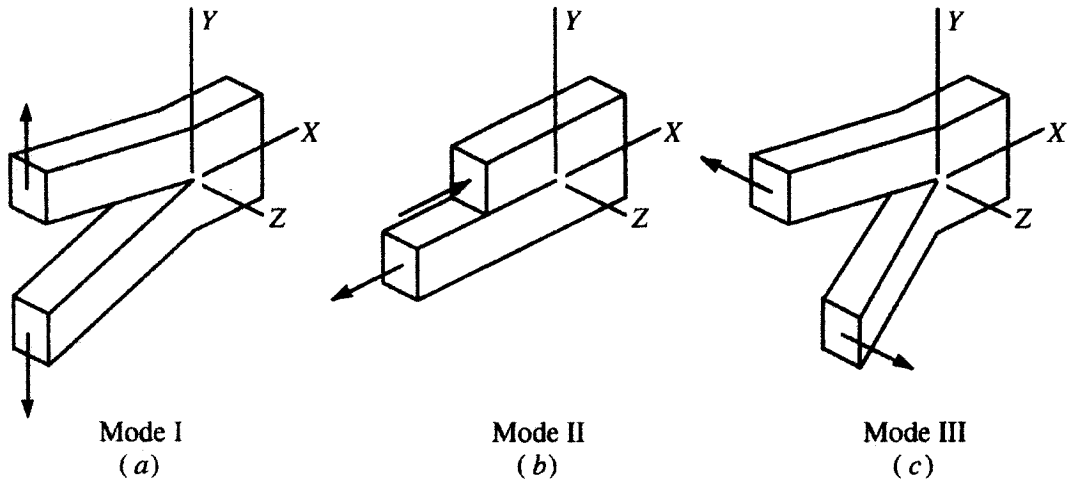


**Figure 11.9** The three modes of failure: (*a*) opening mode, or mode I, characterized by $K_{Ic}$; (*b*) sliding mode, or mode II, $K_{IIc}$; (*c*) tearing mode, or mode III, $K_{IIIc}$.

of scribing a glass plate are quite different from those of a metal one. Thus the question is, what renders brittle solids notch-sensitive, or more directly, why are ceramics brittle?

The answer is related to the crack tip plasticity. In the foregoing discussion, it was assumed that intrinsically brittle fracture was free of crack-tip plasticity, i.e., dislocation generation and motion. Given that dislocations are generated and move under the influence of *shear stresses*, two limiting cases can be considered:

1. The cohesive tensile stress ($\approx Y/10$) is *smaller* than the cohesive strength in shear, in which case the solid can sustain a sharp crack and the Griffith approach is valid.
2. The cohesive tensile stress is *greater* than the cohesive strength in shear, in which case shear breakdown will occur (i.e., dislocations will move away from the crack tip) and the crack will lose its atomic sharpness. In other words, the emission of dislocations from the crack tip, as shown in Fig. 11.10*a*, will move material away from the crack tip, absorbing energy and causing crack blunting, as shown in Fig. 11.10*b*.

Theoretical calculations have shown that the ratio of theoretical shear strength to tensile strength diminishes as one proceeds from covalent to ionic to metallic bonds. For metals, the intrinsic shear strength is so low that flow at ambient temperatures is almost inevitable. Conversely, for covalent materials such as diamond and SiC, the opposite is true: the exceptionally rigid tetrahedral bonds would rather extend in a mode I type of crack than shear.

Theoretically, the situation for ionic solids is less straightforward, but direct observations of crack tips in transmission electron microscopy tend to support the notion that most covalent and ionic solids are truly

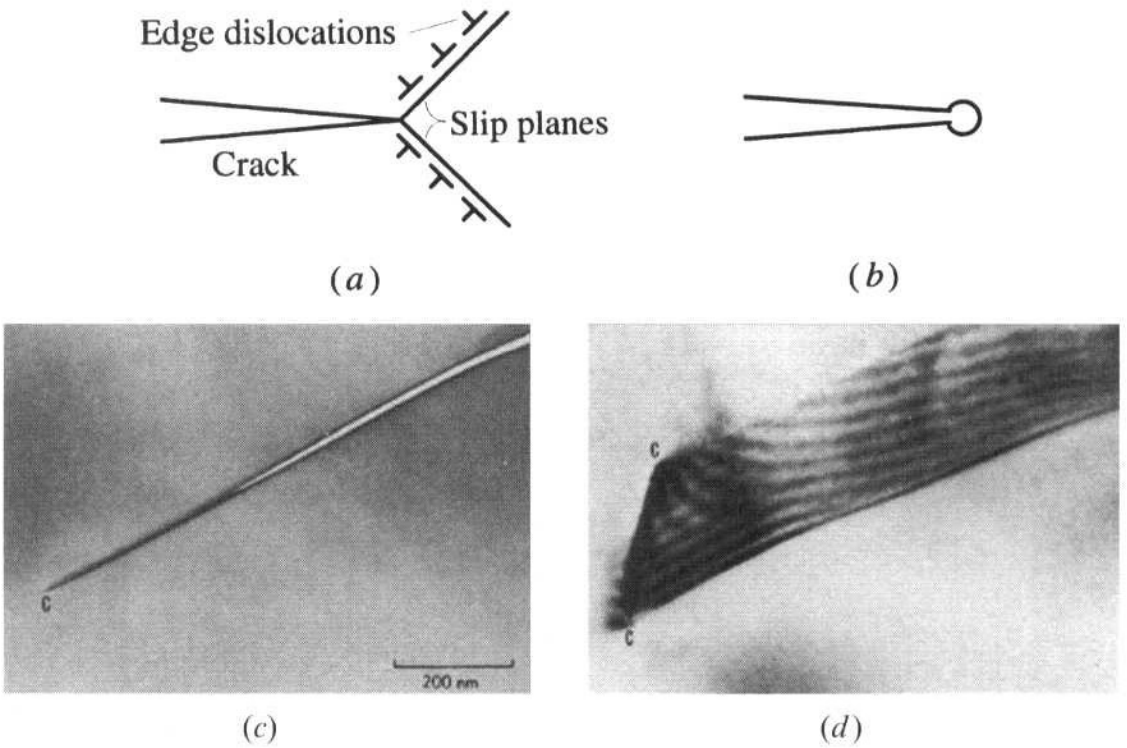


**Figure 11.10** (*a*) Emission of dislocations from crack tip. (*b*) Blunting of crack tip due to dislocation motion. (*c*) Transmission electron micrograph of cracks in Si at 25°C. (*d*) Another crack in Si formed at 500°C, where dislocation activity in vicinity of crack tip is evident.[192]

brittle at room temperature (see Fig. 11.10*c*). Note that the roughly order-of-magnitude difference between the fracture toughness of metals (20 to 100 $MPa \cdot m^{1/2}$) and ceramics is directly related to the lack of crack-tip plasticity in the latter — moving dislocations consumes quite a bit of energy.

The situation is quite different at higher temperatures. Since dislocation mobility is thermally activated, increasing the temperature will tend to favor dislocation activity, as shown in Fig. 11.10*d*, which in turn increases the ductility of the material. Thus the condition for brittleness can be restated as follows: Solids are brittle when the energy barrier for dislocation motion is large relative to the thermal energy $kT$ available to the system. Given the large flow stresses required to move dislocations at elevated temperatures in oxide single crystals (Fig. 11.11), it is once again not surprising that ceramics are brittle at room temperatures. Finally, note that dislocation activity is not the only mechanism for crack blunting. At temperatures above the glass transition temperature viscous flow is also very effective in blunting cracks.

[192] B. R. Lawn, B. J. Hockey, and S. M. Wiederhorn, *J. Mat. Sci.*, **15**:1207 (1980). Reprinted with permission.

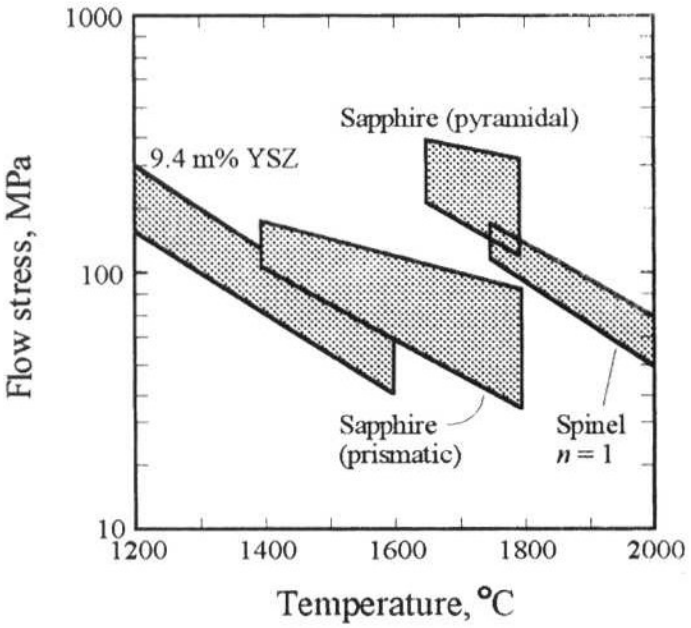


**Figure 11.11** Temperature dependence of flow stress for yttria-stabilized zirconia (YSZ), sapphire, and equimolar spinel.[193]

## 11.3 Strength of Ceramics

Most forming methods that are commonly used in the metal and polymer industries are not applicable for ceramics. Their brittleness precludes deformation methods; and their high melting points, and in some cases (e.g., $Si_3N_4$, SiC) decomposition prior to melting, preclude casting. Consequently, as discussed in the previous chapter, most polycrystalline ceramics are fabricated by either solid- or liquid-phase sintering, which can lead to flaws. For example, how agglomeration and inhomogeneous packing during powder preparation often led to the development of flaws in the sintered body was discussed in Chap. 10. Inevitably, flaws are always present in ceramics. In this section, the various types of flaws that form during processing and their effect on strength are discussed. The subsequent section deals with the effect of grain size on strength, while Sec. 11.3.3 deals briefly with strengthening ceramics by the introduction of compressive surface layers. Before one proceeds much further, however, it is important to briefly review how the strength of a ceramic is measured.

---

### Experimental Details: Modulus of Rupture

Tensile testing of ceramics is time-consuming and expensive because of the difficulty in machining test specimens. Instead, the simpler transverse bending or flexure test is used, where the specimen is loaded to failure in either

[193] A. H. Heuer, cited in R. Raj, *J. Amer. Cer. Soc.*, **76**:2147–2174 (1993).

three- or four-point bending. The maximum stress or stress at fracture is commonly referred to as the *modulus of rupture* (MOR). For rectangular cross sections, the MOR in *four-point* bending is given by

$$\sigma_{\text{MOR}} = \frac{3(S_1 - S_2)F_{\text{fail}}}{2BW^2} \tag{11.15}$$

where $F_{\text{fail}}$ is the load at fracture and all the other symbols are defined in Fig. 11.6*a*. Note that the MOR specimen is unnotched and fails as a result of preexisting surface or interior flaws.

Once again a word of caution: Although the MOR test appears straightforward, it is also fraught with pitfalls.[194] For example, the edges of the samples have to be carefully beveled before testing since sharp corners can act as stress concentrators and in turn significantly reduce the measured strengths.

---

### 11.3.1 Processing and Surface Flaws

The flaws in ceramics can be either internal or surface flaws generated during processing or surface flaws introduced later, during machining or service.

#### Pores

Pores are usually quite deleterious to the strength of ceramics not only because they reduce the cross-sectional area over which the load is applied, but more importantly because they act as stress concentrators. Typically the strength and porosity have been related by the following empirical relationship:

$$\sigma_p = \sigma_0 e^{-BP} \tag{11.16}$$

where $P$, $\sigma_p$, and $\sigma_0$ are, respectively, the volume fraction porosity and the strength of the specimen with and without porosity; $B$ is a constant that depends on the distribution and morphology of the pores. The exponential dependence of strength on porosity is clearly demonstrated in Fig. 11.12 for reaction-bonded $Si_3N_4$, which is formed by exposing a Si compact to a nitrogen atmosphere at elevated temperatures. The large scatter in the results mostly reflects the variability in the pore sizes, morphology, and distribution.

Usually, the stress intensities associated with the pores themselves are insufficient to cause failure, and as such the role of pores is indirect. Fracture from pores is typically dictated by the presence of other defects in their immediate vicinity. If the pore is much larger than the surrounding grains, atomically sharp cusps around the surface of the former can result. The critical flaw thus becomes comparable to the dimension of the pores. If the

[194] For a comprehensive review of the MOR test, see G. Quinn and R. Morrell, *J. Am. Cer. Soc.*, **74**(9):2037–2066 (1991).

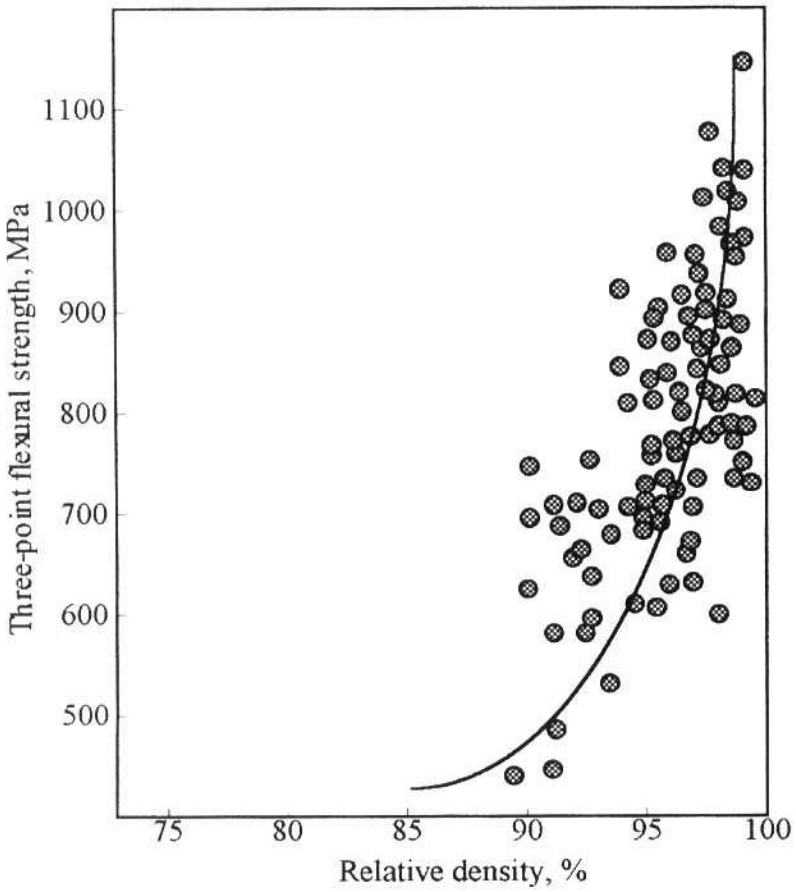


**Figure 11.12** Functional dependence of strength on porosity for a reaction-bonded $Si_3N_4$.[195]

pores are spherical, as in glasses, they are less detrimental to the strength. Thus both the largest dimension of the pore and the smallest radius of curvature at the pore surface are what determines their effect on the strength. A typical micrograph of a pore that resulted in failure is shown in Fig. 11.13*a*.

## Inclusions

Impurities in the starting powders can react with the matrix and form inclusions that can have different mechanical and thermal properties from the original matrix. Consequently, as a result of the mismatch in the thermal expansion coefficients of the matrix $\alpha_m$ and the inclusions $\alpha_i$, large residual stresses can develop as the part is cooled from the processing temperature. For example, a spherical inclusion of radius $R$ in an infinite matrix will result in both radial ($\sigma_{rad}$) and tangential ($\sigma_{tan}$) residual stresses at a radial distance $r$ away from the inclusion/matrix interface given by

$$\sigma_{rad} = -2\sigma_{tan} = \frac{(\alpha_m - \alpha_i)\Delta T}{[(1-2\nu_i)/Y_i + (1+\nu_m)/2Y_m]}\left(\frac{R}{r+R}\right)^3 \qquad (11.17)$$

[195] Data taken from O. Kamigaito, in *Fine Ceramics*, S. Saito, ed., Elsevier, New York, 1988.

where $\nu$ is Poisson's ratio; $m$ and $i$ refer to the matrix and inclusion, respectively; and $\Delta T$ is the difference between the initial and final temperatures (i.e., it is defined as positive during cooling and negative during heating). On cooling, the initial temperature is the maximum temperature below which the stresses are not relaxed. (See Chap. 13 for more details.)

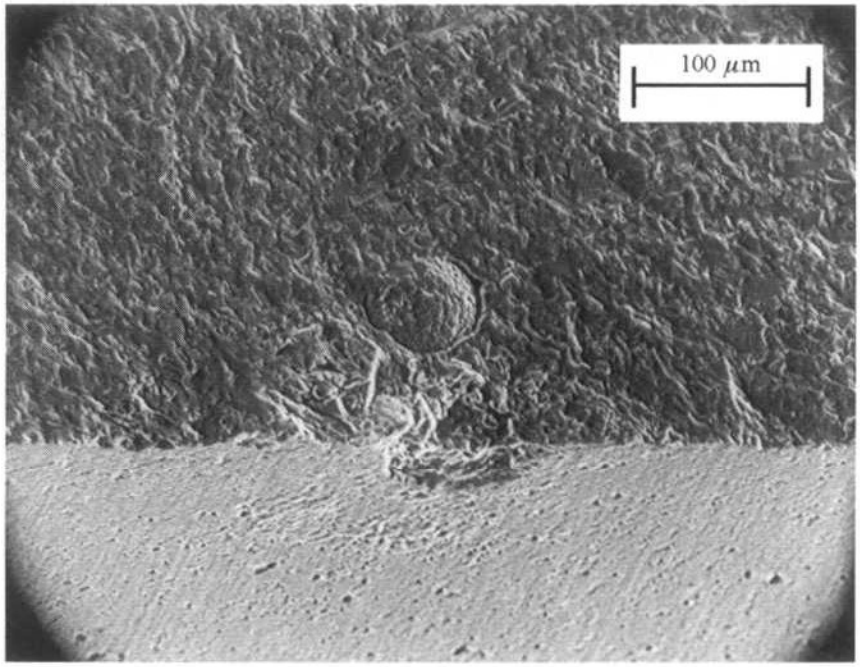


(*a*)

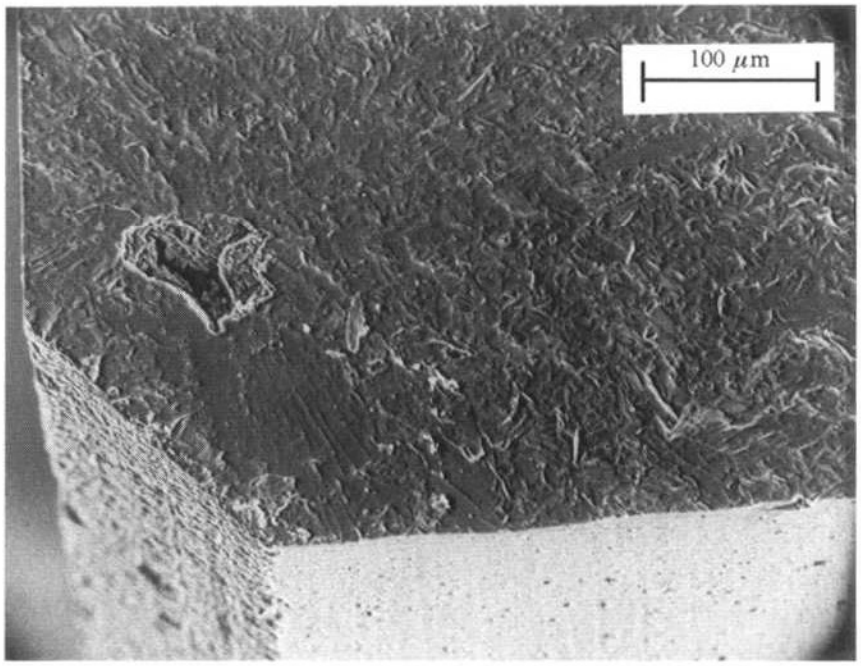


(*b*)

**Figure 11.13** (*a*) Large pore associated with a large grain in sintered α-SiC. (*b*) An agglomerate with associated porosity in a sintered α-SiC.[196]

[196] G. Quinn and R. Morrell, *J. Am. Cer. Soc.*, **74**(9):2037–2066 (1991). Reprinted with permission.

It follows from Eq. (11.17) that upon cooling, if $\alpha_i < \alpha_m$, large tangential tensile stresses develop that, in turn, could result in the formation of radial matrix cracks. Conversely, if $\alpha_i > \alpha_m$, the inclusion will tend to detach itself from the matrix and produce a porelike flaw.

**Agglomerates and large grains**

The rapid densification of regions containing fine particles (agglomerates) can induce stresses within the surrounding compact. Voids and cracks usually tend to form around agglomerates, as shown in Fig. 11.13*b*. These voids form as a result of the rapid and large differential shrinkage of the agglomerates during the early stages of sintering. Since these agglomerates form during the fabrication of the green bodies, care must be taken at that stage to avoid them.

Similarly, large grains caused by exaggerated grain growth during sintering often result in a degradation in strength. Large grains, if noncubic, will be anisotropic with respect to such properties as thermal expansion and elastic modulus, and their presence in a fine-grained matrix essentially can act as inclusions in an otherwise homogeneous matrix. The degradation in strength is also believed to be partly due to residual stresses at grain boundaries that result from thermal expansion mismatches between the large grains and the surrounding matrix. The magnitude of the residual stresses will depend on the grain shape factor and the grain size, but can be approximated by Eq. (11.17). The effect of grain size on the residual stresses and spontaneous microcracking will be dealt with in greater detail in Chap. 13.

**Surface flaws**

Surface flaws can be introduced in a ceramic as a result of high-temperature grain boundary grooving, postfabrication machining operations, or accidental damage to the surface during use, among others. During grinding, polishing, or machining, the grinding particles act as indenters that introduce flaws into the surface. These cracks can propagate through a grain along cleavage planes or along the grain boundaries, as shown in Fig. 11.14. In either case, the cracks do not extend much farther than one grain diameter before they are usually arrested. The machining damage thus penetrates approximately one grain diameter from the surface. Consequently, according to the Griffith criterion, the fracture stress is expected to decrease with increasing grain size — an observation that is commonly observed. This brings up the next important topic, which relates the strength of ceramics to their grain size.

### 11.3.2 Effect of Grain Size on Strength

Typically, the strength of ceramics shows an inverse correlation to the average grain size $G$. A schematic of the dependence is shown in

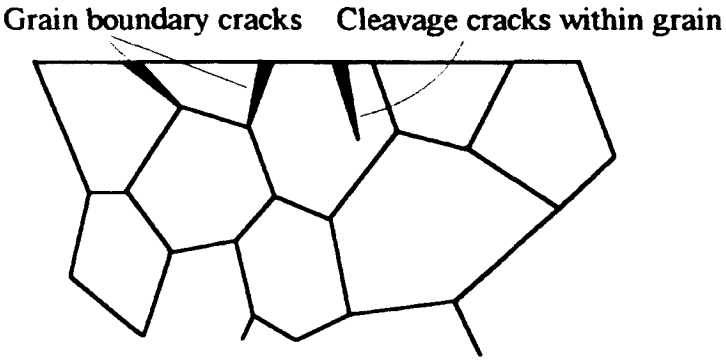


**Figure 11.14** Schematic of cleavage and grain boundary cracks that can form on the surface of ceramics as a result of machining. The flaws are usually limited to one grain diameter, however, because they are deflected at the grain boundaries.

Fig. 11.15*a*, where the fracture strength is plotted versus $G^{-1/2}$. The simplest explanation for this behavior is that the intrinsic flaw size scales with the grain size, a situation not unlike the one shown in Fig. 11.14. The flaws form at the grain boundaries, which are weak areas to begin with, and propagate up to about one grain diameter. Thus once more invoking the Griffith criterion, one expects the strength to be proportional to $G^{-1/2}$, as is observed. It is worth noting that the strength does not keep on increasing with decreasing grain size. For very fine-grained ceramics, fracture usually occurs from preexistent process or surface flaws in the material, and thus the strength becomes relatively grain-size-insensitive. In other

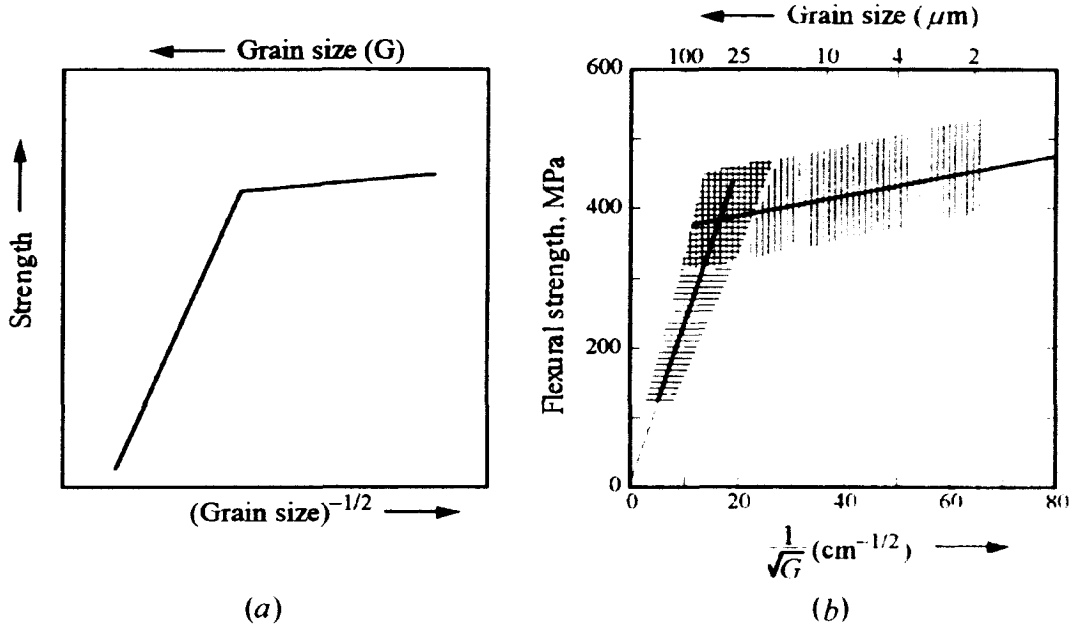


**Figure 11.15** (*a*) Schematic relationship between grain size and strength for a number of ceramics. (*b*) Actual data for $MgAl_2O_4$. Courtesy of R. W. Rice.

words, the line shown in Fig. 11.15 becomes much less steep for smaller grain sizes.

### 11.3.3 Effect of Compressive Surface Residual Stresses

The introduction of surface compressive layers can strengthen ceramics and is a well-established technique for glasses (see Sec. 13.5 for more details). The underlying principle is to introduce a state of compressive surface residual stress, the presence of which would inhibit failure from surface flaws since these compressive stresses would have to be overcome before a surface crack could propagate. These compressive stresses have also been shown to enhance thermal shock resistance and contact damage resistance.

There are several approaches to introducing a state of compressive residual stress, but in all cases the principle is to generate a surface layer with a higher volume than the original matrix. This can be accomplished in a variety of ways:

- Incorporation of an outer layer having a lower coefficient of thermal expansion, as in glazing or tempering of glass. These will be discussed in greater detail in Chap. 13.
- Using transformation stresses in certain zirconia ceramics (see next section).
- Physically stuffing the outer layer with atoms or ions such as by ion implantation.
- Ion-exchanging smaller ions for larger ions. The larger ions that go into the matrix place the latter in a state of compression. This is similar to physical stuffing and is most commonly used in glasses by placing a glass in a molten salt that contains the larger ions. The smaller ions are exchanged by the larger ions, which in turn place the surface in compression.

One aspect of this technique is that to balance the compressive surface stresses, a tensile stress develops in the center of the part. Thus if a flaw actually propagates through the compressive layer, the material is then weaker than in the absence of the compressive layer, and the release of the residual stresses can actually cause the glass to shatter. This is the principle at work in the manufacture of tempered glass for car windshields which upon impact shatter into a large number of small pieces that are much less dangerous than larger shards of glass, which can be lethal.

### 11.3.4 Effect of Temperature on Strength

The effect of temperature on the strength of ceramics depends on many factors, the most important of which is whether the atmosphere in which the testing is being carried out heals or exacerbates preexisting surface flaws in the material. In general, when a ceramic is exposed to a corrosive

atmosphere at elevated temperatures, one of two scenarios is possible: (1) A protective, usually oxide, layer forms on the surface, which tends to blunt and partially heal preexisting flaws and can result in an increase in the strength. (2) The atmosphere attacks the surface, either forming pits on the surface or simply etching the surface away at selective areas; in either case, a drop in strength is observed. For ceramics containing glassy grain boundary phases, at high enough temperatures the drop in strength is usually related to the softening of these phases.

## 11.4 Toughening Mechanisms

Despite the fact that ceramics are inherently brittle, a variety of approaches have been used to enhance their fracture toughness and resistance to fracture. The essential idea behind all toughening mechanisms is to increase the energy needed to extend a crack, that is, $G_c$ in Eq. (11.11). The basic approaches are crack deflection, crack bridging, and transformation toughening.

### 11.4.1 Crack Deflection

It is experimentally well established that the fracture toughness of a polycrystalline ceramic is appreciably higher than that of single crystals of the same composition. For example, $K_{Ic}$ of single-crystal alumina is about $2.2\,\text{MPa}\cdot\text{m}^{1/2}$, whereas that for polycrystalline alumina is closer to $4\,\text{MPa}\cdot\text{m}^{1/2}$. Similarly, the fracture toughness of glass is $\approx 0.8\,\text{MPa}\cdot\text{m}^{1/2}$, whereas the fracture toughness of a glass-ceramic of the same composition is closer to $2\,\text{MPa}\cdot\text{m}^{1/2}$. One of the reasons invoked to explain this effect is crack deflection at the grain boundaries, a process illustrated in Fig. 11.16*a*. In a polycrystalline material, as the crack is deflected along the weak grain boundaries, the average stress intensity at its tip $K_{tip}$ is reduced, because the stress is no longer always normal to the crack plane [an implicit assumption made in deriving Eq. (11.9)]. In general, it can be shown that $K_{tip}$ is related to the applied stress intensity $K_{app}$ and the angle of deflection, $\theta$ (defined in Fig. 11.16*a*), by

$$K_{tip} = \left(\cos^3 \frac{\theta}{2}\right) K_{app} \tag{11.18}$$

Based on this equation, and assuming an average $\theta$ value of, say, 45°, the increase in fracture toughness expected should be about 1.25 above the single-crystal value. By comparing this conclusion with the experimental results listed above, it is clear that crack deflection by itself accounts for some of, but not all, the enhanced toughening. In polycrystalline materials, crack bifurcation around grains can lead to a much more potent toughening mechanism, namely, crack bridging — the topic tackled next.

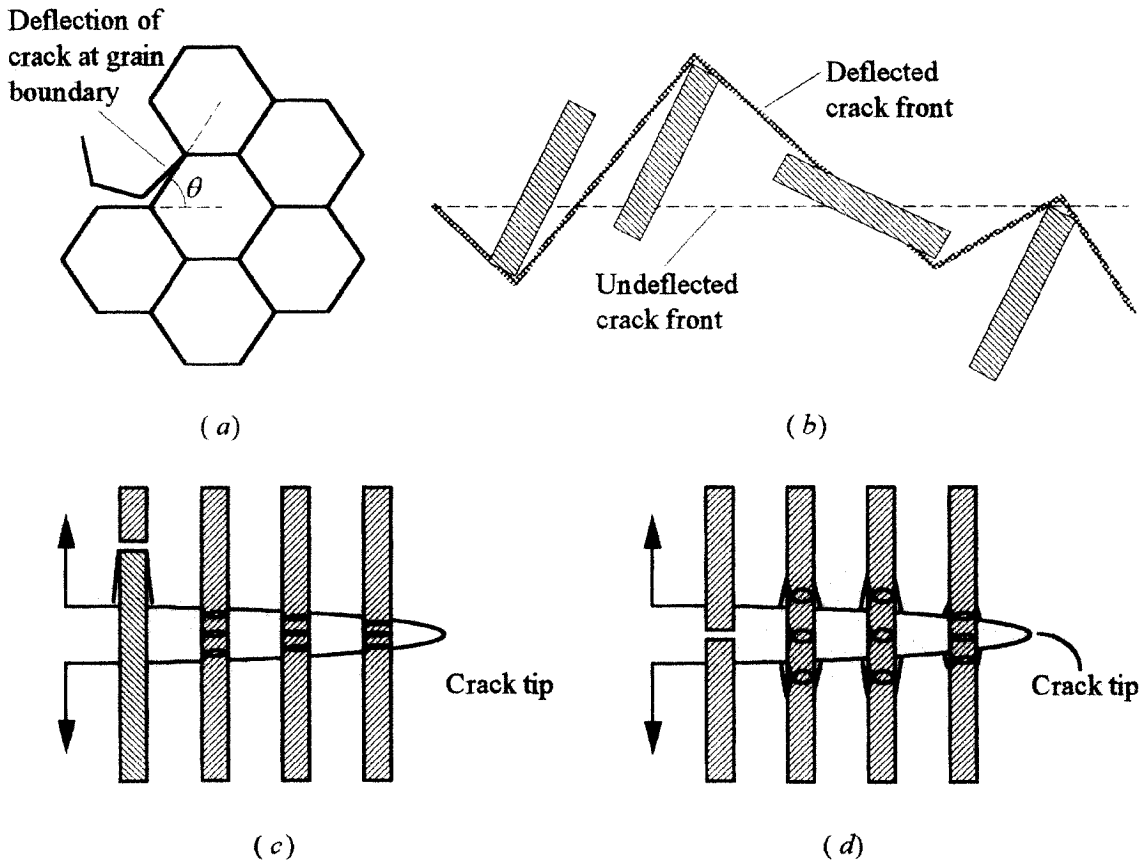


**Figure 11.16** (*a*) Schematic of crack deflection mechanism at grain boundaries. (*b*) Schematic indicating deflection of crack front around rod-shaped particles.[197] (*c*) Schematic of ligament bridging mechanism with no interfacial debonding and (*d*) with debonding. Note that in this case the strain on the ligaments is delocalized, and the toughening effect is enhanced.

### 11.4.2 Crack Bridging

In this mechanism, the toughening results from bridging of the crack surfaces behind the crack tip by a strong reinforcing phase. These bridging ligaments (Fig. 11.16*b* and *c*) generate closure forces on the crack face that reduce $K_{tip}$. In other words, by providing some partial support of the applied load, the bridging constituent reduces the crack-tip stress intensity. The nature of the ligaments varies but they can be whiskers, continuous fibers (Fig. 11.16*c*), or elongated grains (Fig. 11.16*b*). A schematic of how these elastic ligaments result in a closure force is seen in Fig. 11.16*c*. A useful way to think of the problem is to imagine the unbroken ligaments in the crack wake as tiny springs that have to be stretched, and hence consume energy, as the crack front advances.

[197] Adapted from A. G. Evans and R. M. Cannon, *Acta. Met.*, **34**:761 (1986).

It can be shown that the fracture toughness of a composite due to elastic stretching of a partially debonded reinforcing phase at the crack tip with no interfacial friction is given by[198]

$$K_{Ic} = \sqrt{Y_c G_m + \sigma_f^2 \left( \frac{r V_f Y_c \gamma_f}{12 Y_f \gamma_i} \right)} \tag{11.19}$$

where the subscripts $c$, $m$, and $f$ represent the composite, matrix, and reinforcement, respectively; $Y$, $V$, and $\sigma_f$ are the Young's modulus, volume fraction, and strength of the reinforcement phases, respectively; $r$ is the radius of the bridging ligament, and $G_m$ is the toughness of the unreinforced matrix; and $\gamma_f/\gamma_i$ represents the ratio of the fracture energy of the bridging ligaments to that of the reinforcement/matrix interface. Equation (11.19) predicts that the fracture toughness increases with

- Increasing fiber volume fraction of reinforcing phase
- Increasing $Y_c/Y_f$ ratio
- Increasing $\gamma_f/\gamma_i$ ratio (i.e., the toughness is enhanced for weak fiber matrix interfaces)

Comparing Fig. 11.16*c* and *d* reveals how the formation of a debonded interface spreads the strain displacement imposed on the bridging reinforcing ligament over a longer gauge length. As a result, the stress supported by the ligaments increases more slowly with distance behind the crack tip, and greater crack-opening displacements are achieved in the bridging zone, which in turn significantly enhances the fracture resistance of the composite. An essential ingredient of persistent bridge activity is that substantial pullout can occur well after whisker rupture. The fiber bridging mechanism is thus usually supplemented by a contribution of pullout of the reinforcement from fibers that fail away from the crack plane (Fig. 11.16*c*). As the ligaments pull out of the matrix, they consume energy that has to be supplied to the advancing crack, further enhancing the toughness of the composite.

That toughening contributions obtained by crack bridging and pullout can yield substantially increased fracture toughness is demonstrated in Fig. 11.17*a* for a number of whisker-reinforced ceramics. The solid lines are predicted curves and the data points are the experimental results; the agreement is quite good. A similar mechanism accounts for the high toughnesses achieved recently in $Si_3N_4$ with acicular grains (Fig. 11.17*b*), coarser grain-sized aluminas, and other ceramics.

### 11.4.3 Transformation Toughening

Transformation-toughened materials owe their very large toughness to the stress-induced transformation of a metastable phase in the vicinity of a

[198] See, e.g., P. Becher, *J. Amer. Cer. Soc.*, **74**:255–269 (1991).

propagating crack. Since the original discovery[199] that the tetragonal-to-monoclinic ($t \Rightarrow m$) transformation of zirconia (see Chap. 8) has the potential for increasing both the fracture stress and the toughness of zirconia and zirconia-containing ceramics, a large effort has been dedicated to understanding the phenomenon.[200]

To understand the phenomenon, it is useful to refer to Fig. 11.18, where fine tetragonal zirconia grains are dispersed in a matrix. If these tetragonal

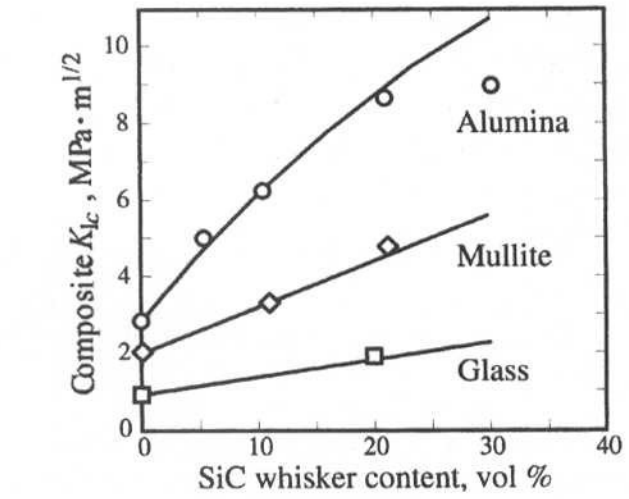


(*a*)

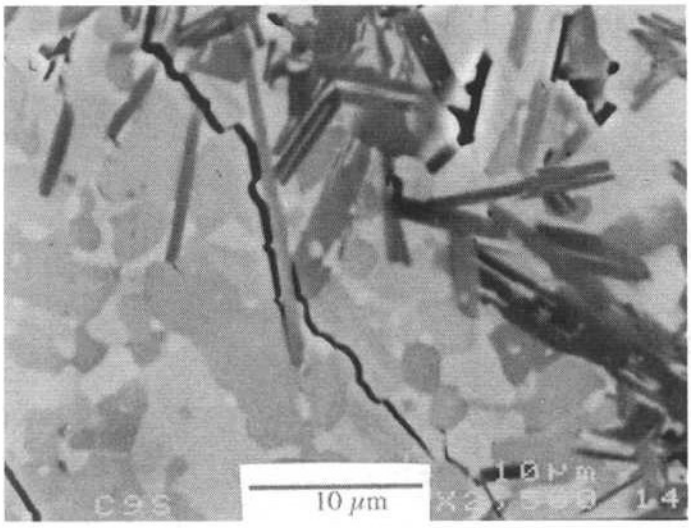


(*b*)

**Figure 11.17** (*a*) The effect of SiC whisker content on toughness enhancement in different matrices.[201] (*b*) Toughening is associated with crack bridging and grain pullout of elongated matrix grains.

[199] R. Garvie, R. Hannick, and R. Pascoe, *Nature*, **258**:703 (1975).

[200] See, e.g., A. G. Evans and R. M. Cannon, *Acta. Metall.*,**34**:761–800 (1986). For more recent work, see D. Marshall, M. Shaw, R. Dauskardt, R. Ritchie, M. Ready, and A. Heuer, *J. Amer. Cer. Soc.*, **73**:2659–2666 (1990).

[201] P. Becher, "Microstructural Design of Toughened Ceramics," *J. Amer. Cer. Soc.*, **74**:255–269 (1991).

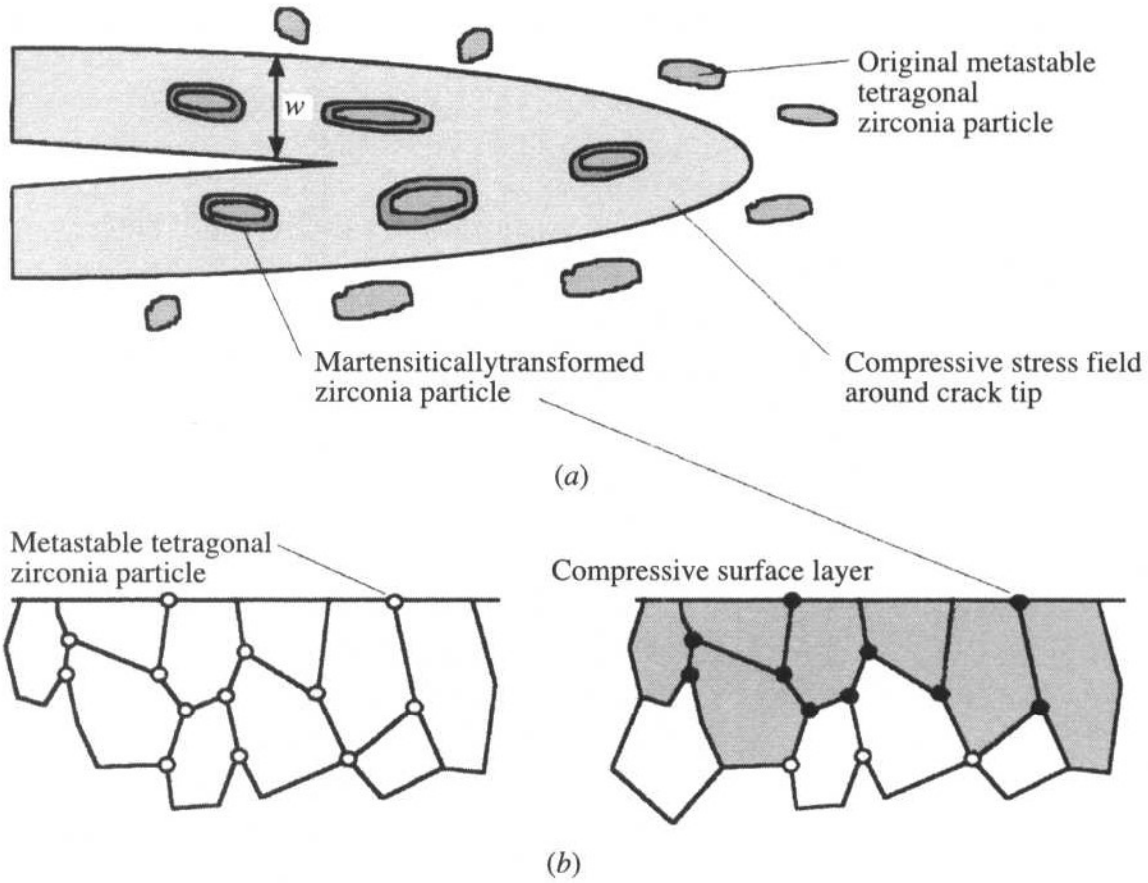


**Figure 11.18** (*a*) Transformation zone ahead and around crack tip. (*b*) Surface grinding induces the martensitic transformation, which in turn creates compressive surface layers and a concomitant increase in strength.

particles are fine enough, then upon cooling from the processing temperatures, they can be constrained from transforming by the surrounding matrix and consequently can be retained in a *metastable tetragonal phase*. If, for any reason, that constraint is lost, the transformation — which is accompanied by a relatively large volume expansion or dilatation ($\approx$4 percent) and shear strain ($\approx$7 percent) — is induced. In transformation toughening, the approaching crack front, being a free surface, is the catalyst that triggers the transformation, which in turn places the zone ahead of the crack tip in compression. Given that the transformation occurs in the vicinity of the crack tip, extra energy is required to extend the crack through that compressive layer, which increases both the toughness and the strength of the ceramic.

The effect of the dilation strains is to reduce the stress intensity at the crack tip $K_{\text{tip}}$ by a shielding factor $K_s$ such that

$$K_{\text{tip}} = K_a - K_s \tag{11.20}$$

It can be shown that if the zone ahead of the crack tip contains a uniform volume fraction $V_f$ of transformable phase that transforms in a

zone of width $w$, shown in Fig. 11.18*a*, from the crack surface, then the shielding crack intensity factor is given by[202]

$$K_s = A' Y V_f \varepsilon^T \sqrt{w} \tag{11.21}$$

where $A'$ is a dimensionless constant on the order of unity that depends on the shape of the zone ahead of the crack tip and $\varepsilon^T$ is the transformation strain. A methodology to calculate $\varepsilon^T$ is discussed in Chap. 13.

Fracture will still occur when $K_{\text{tip}} = K_{Ic}$ of the matrix in the absence of shielding; however, now the enhanced fracture toughness comes about by the shielding of $K_{\text{tip}}$ by $K_s$. Careful microstructural characterization of crack-tip zones in various zirconias has revealed that the enhancement in fracture toughness does in fact scale with the product $V_f \sqrt{w}$, consistent with Eq. (11.21).

It is unfortunate that the reason transformation toughening works so well at ambient temperatures — mainly the metastability of the tetragonal phase — is the same reason it is ineffective at elevated temperatures. Increasing the temperature reduces the driving force for transformation and consequently the extent of the transformed zone, leading to less tough materials.

It is worth noting that the transformation can be induced any time the hydrostatic constraint of the matrix on the metastable particles is relaxed. For example, it is now well established that compressive surface layers are developed as a result of the spontaneous transformation. The process is shown schematically in Fig. 11.18*b*. The fracture strength can be almost doubled by simply abrading the surface, since surface grinding has been shown to be an effective method for inducing the transformation. Practically this is important, because we now have a ceramic that, in principle, becomes stronger as it is handled and small scratches are introduced on its surface.

At this stage, three classes of toughened zirconia-containing ceramics have been identified:

- *Partially stabilized zirconia* (PSZ). In this material the cubic phase is less than totally stabilized by the addition of MgO, CaO, or $Y_2O_3$. The cubic phase is then heat-treated to form coherent tetragonal precipitates. The heat treatment is such as to keep the precipitates small enough so they do not spontaneously transform within the cubic zirconia matrix but only as a result of stress.
- *Tetragonal zirconia polycrystals* (TZPs). These ceramics contain 100 percent tetragonal phase and small amounts of yttria and other rare-earth additives. With bend strength exceeding 2000 MPa, these ceramics are among the strongest known.

[202] R. M. McMeeking and A. G. Evans, *J. Amer. Cer. Soc.*, **63**:242–246 (1982).

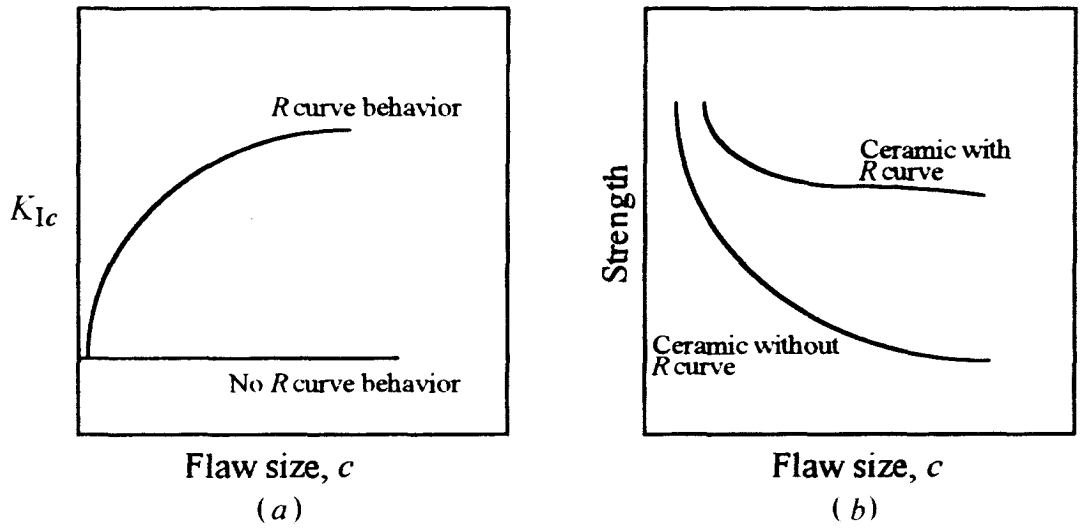


**Figure 11.19** (*a*) Functional dependence of fracture toughness on flaw size for a ceramic exhibiting *R* curve behavior (top curve) and one that does not (lower curve). (*b*) Effect of *R* curve behavior on strength degradation as flaw size increases. Ceramics exhibiting *R* curve behavior are more flaw-tolerant than those that do not.

- *Zirconia-toughened ceramics* (ZTCs). These consist of tetragonal or monoclinic zirconia particles finely dispersed in other ceramic matrices such as alumina, mullite, and spinel.

### 11.4.4 *R* Curve Behavior

One of the important consequences of the toughening mechanisms described above is that they result in what is known as *R curve behavior*. In contrast to a typical Griffith solid where the fracture toughness is independent of crack size, *R* curve behavior refers to a fracture toughness which increases as the crack grows, as shown schematically in Fig. 11.19*a*. The main mechanisms responsible for this type of behavior are the same as those operative during crack bridging or transformation toughening, i.e., the closure forces imposed by either the transformed zone or the bridging ligaments. For example, referring once again to Fig. 11.16*c*, one sees that as the number of bridging ligaments increases in the crack wake, so will the energy required to extend the crack. The fracture toughness does not increase indefinitely, however, but reaches a plateau when the number of ligaments in the crack wake reach a steady-state with increasing crack extension. Further away from the crack tip, the ligaments tend to break and pull out completely and thus become ineffective.

There are four important implications for ceramics that exhibit *R* curve behavior:

1. The degradation in strength with increasing flaw size is less severe for ceramics without *R* curve behavior. This is shown schematically in Fig. 11.19*b*.

2. The reliability of the ceramic increases. This will be discussed in detail in Sec. 11.5.
3. On the down side, there is now an increasing body of evidence that seems to indicate that ceramics that exhibit $R$ curve behavior are more susceptible to fatigue than ceramics that do not exhibit $R$ curve behavior. This is discussed in greater detail in Chap. 12.
4. There is some recent evidence to suggest that $R$ curve behavior enhances the thermal shock resistance of some ceramics. The evidence at this point is not conclusive, however, and more work is needed in this area.

To summarize, fracture toughness is related to the work required to extend a crack and is determined by the details of the crack propagation process. Only for the fracture of the most brittle solids is the fracture toughness simply related to surface energy. The fracture toughness can be enhanced by increasing the energy required to extend the crack. Crack bridging and martensitic transformations are two mechanisms that have been shown to enhance $K_{Ic}$.

## 11.5 Designing With Ceramics

In light of the preceding discussion, one expects that the failure stress, being as sensitive as it is to flaw sizes and their distributions, will exhibit considerable variability or scatter. This begs the question: Given this variability, is it still possible to design critical load-bearing parts with ceramics? In theory, if the flaws in a part were fully characterized (i.e., their size and orientation with respect to the applied stresses) and the stress concentration at each crack tip could be calculated, then given $K_{Ic}$, the exact stress at which a component would fail could be determined, and the answer to the question would be yes. Needless to say, such a procedure is quite impractical for several reasons, least among them the difficulty of characterizing all the flaws inside a material and the time and effort that would entail.

An alternative approach, described below, is to characterize the behavior of a large number of samples of the same material and to use a statistical approach to design. Having to treat the problem statistically has far-reaching implications since now the best that can be hoped for in designing with brittle solids is to state the *probability* of survival of a part at a given stress. The design engineer must then assess an acceptable risk factor and, using the distribution parameters described below, estimate the appropriate design stress.

Other approaches being taken to increase the reliability of ceramics are nondestructive testing and proof testing. The latter approach is briefly discussed in Sec. 11.5.2.

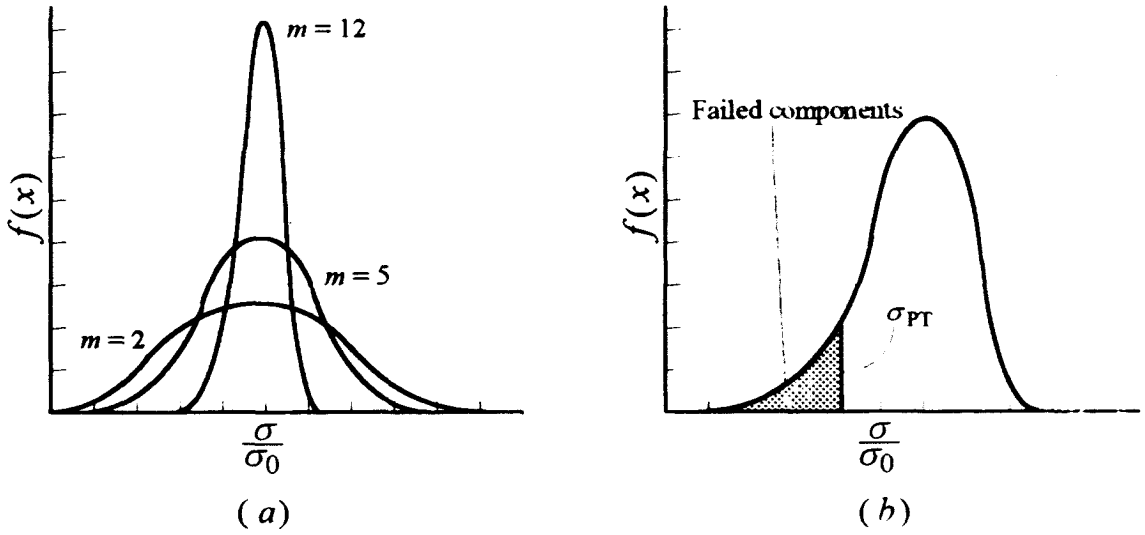


**Figure 11.20** (*a*) The effect of $m$ on the shape of the Weibull distribution. As $m$ increases, the distribution narrows. (*b*) Truncation of Weibull distribution as a result of proof testing.

### 11.5.1 The Statistical Approach

#### Weibull distributions

One can describe the strength distribution of a ceramic in a variety of formalisms. The one most widely used today is the *Weibull distribution.*[203] This two-parameter semiempirical distribution is given by

$$f(x) = m(x)^{m-1} \exp(-x^m) \tag{11.22}$$

where $f(x)$ is the frequency distribution of the random variable $x$ and $m$ is a shape factor, usually referred to as the *Weibull modulus.* When Eq. (11.22) is plotted (see Fig. 11.20*a*), a bell-shaped curve results, the width of which depends on $m$; as $m$ gets larger, the distribution narrows.

Since one is dealing with a strength distribution, the random variable $x$ is defined as $\sigma/\sigma_0$, where $\sigma$ is the failure stress and $\sigma_0$ is a normalizing parameter, required to render $x$ dimensionless and whose physical significance will be discussed shortly.

Replacing $x$ by $\sigma/\sigma_0$ in Eq. (11.22), one finds the survival probability, i.e., the fraction of samples that would survive a given stress level, is simply

$$S = \int_{\sigma/\sigma_0}^{\infty} f\left(\frac{\sigma}{\sigma_0}\right) d\left(\frac{\sigma}{\sigma_0}\right)$$

or

$$S = \exp\left[-\left(\frac{\sigma}{\sigma_0}\right)^m\right] \tag{11.23}$$

[203] W. Weibull, *J. Appl. Mech.*, **18**:293–297 (1951); *Mat. Res. & Stds.*, May 1962, pp. 405–411.

Rewriting Eq. (11.23) as $1/S = \exp(\sigma/\sigma_0)^m$ and taking the natural log of both sides twice yields

$$\ln \ln \frac{1}{S} = m \ln \frac{\sigma}{\sigma_0} = m \ln \sigma - m \ln \sigma_0 \tag{11.24}$$

Multiplying both sides of Eq. (11.24) by $-1$ and plotting $-\ln \ln(1/S)$ versus $\ln \sigma$ yield a straight line with slope $-m$. The physical significance of $\sigma_0$ is now also obvious: It is the stress level at which the survival probability is equal to $1/e$, or 0.37. Once $m$ and $\sigma_0$ are determined from the set of experimental results, the survival probability at any stress can be easily calculated from Eq. (11.23) (see Worked Example 11.2).

The use of Weibull plots for design purposes has to be handled with extreme care. As with all extrapolations, a small uncertainty in the slope can result in large uncertainties in the survival probabilities, and hence to increase the confidence level, the data sample has to be sufficiently large ($N > 100$). Furthermore, in the Weibull model, it is implicitly assumed that the material is homogeneous, with a single flaw population that does not change with time. It further assumes that only one failure mechanism is operative and that the defects are randomly distributed and are small relative to the specimen or component size. Needless to say, whenever any of these assumptions is invalid, Eq. (11.23) has to be modified. For instance, bimodal distributions that lead to strong deviations from a linear Weibull plot are not uncommon.

**WORKED EXAMPLE 11.2**

The strengths of 10 nominally identical ceramic bars were measured and found to be 387, 350, 300, 420, 400, 367, 410, 340, 345, and 310 MPa. (*a*) Determine $m$ and $\sigma_0$ for this material. (*b*) Calculate the design stress that would ensure a survival probability higher than 0.999.

**Answer**

(*a*) To determine $m$ and $\sigma_0$, the Weibull plot for this set of data has to be made. Do as follows:

- Rank the specimens in order of increasing strength, $1, 2, 3, \ldots, j, j+1, \ldots, N$, where $N$ is the total number of samples.
- Determine the survival probability for the $j$th specimen. As a first approximation, the probability of survival of the first specimen is $1 - 1/(N+1)$; for the second, $1 - 2/(N+1)$, for the $j$th specimen $1 - j/(N+1)$, etc. This expression is adequate for most applications. However, an alternate and more accurate expression deduced from a more detailed statistical analysis yields

$$S_j = 1 - \frac{j - 0.3}{N + 0.4} \tag{11.25}$$

- Plot $-\ln\ln(1/S)$ versus $\ln\sigma$. The least-squares fit to the resulting line is the Weibull modulus.

The last two columns in Table 11.2 are plotted in Fig. 11.21. A least-squares fit of the data yields a slope of 10.5, which is typical of many conventional as-finished ceramics. From the table, $\sigma_0 \approx 385$ MPa (i.e. when $-\ln\ln 1/S = 0$).

**Table 11.2** Summary of data needed to find $m$ from a set of experimental results

| Rank $j$ | $S_j$ | $\sigma_j$ | $\ln\sigma_j$ | $-\ln\ln(1\sigma_j)$ |
|---|---|---|---|---|
| 1 | 0.932 | 300 | 5.700 | 2.6532 |
| 2 | 0.837 | 310 | 5.734 | 1.7260 |
| 3 | 0.740 | 340 | 5.823 | 1.2000 |
| 4 | 0.644 | 345 | 5.840 | 0.8200 |
| 5 | 0.548 | 350 | 5.860 | 0.5080 |
| 6 | 0.452 | 367 | 5.905 | 0.2310 |
| 7 | 0.356 | 387 | 5.960 | −0.0320 |
| 8 | 0.260 | 400 | 5.990 | −0.2980 |
| 9 | 0.160 | 410 | 6.016 | −0.6060 |
| 10 | 0.070 | 420 | 6.040 | −0.9780 |

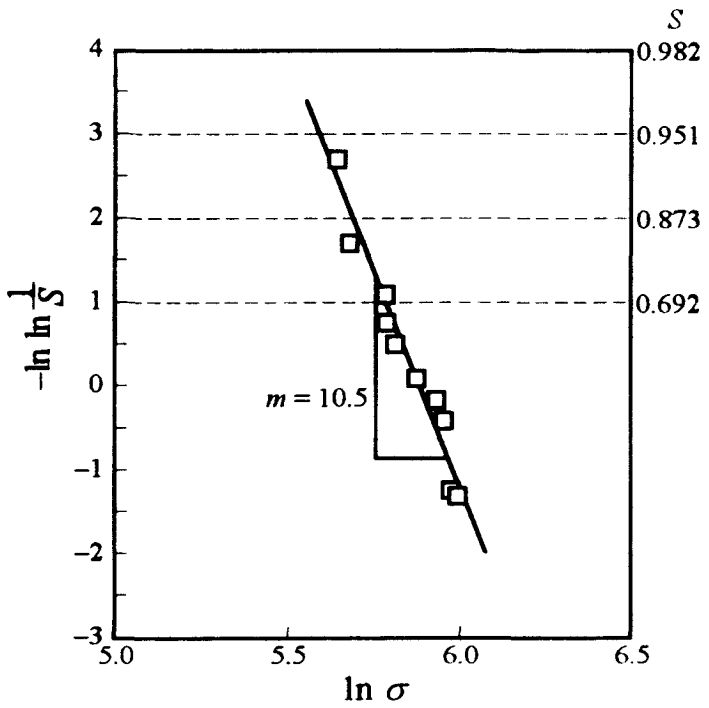


**Figure 11.21** Weibull plot of data shown in Table 11.2. Slope of the line is the Weibull modulus $m$. The actual survival probability is shown on the right-hand side. At low stresses, $S$ is large (left-hand corner of figure).[204]

[204] The reason that $-\ln\ln(1/S)$ is plotted rather than $\ln\ln(1/S)$ is aesthetic, such that the high survival probabilities appear on the upper left-hand sides of the plots.

(*b*) To calculate the stress at which the survival probability is 0.999, use Eq. (11.23), or

$$0.999 = \exp\left\{-\left(\frac{\sigma}{385}\right)^{10.5}\right\}$$

from which $\sigma = 200$ MPa. It is worth noting here that the error in using the average stress of 366 MPa instead of $\sigma_0$ changes the end result for the design stress only slightly. For most applications, it is sufficient to simply use the average stress.

### Factors affecting the Weibull modulus

Clearly, from a design point of view, it is important to have high $m$'s. Note that $m$ should not be confused with strength, since it is possible to have a weak solid with a high $m$ and vice versa. For instance, a solid with large defects that are all identical in size would be weak but, in principle, would exhibit large $m$. It is the *uniformity* of the microstructure, including flaws, grain size, and inclusions, that is critical for obtaining large $m$ values.

Interestingly enough, increasing the fracture toughness for a truly brittle material will not increase $m$. This can be shown as follows: By recasting Eq. (11.24), $m$ can be rewritten as

$$m = \frac{\ln\ln(1/S_{\max}) - \ln\ln(1/S_{\min})}{\ln(\sigma_{\max}/\sigma_{\min})} \tag{11.26}$$

For any set of samples, the numerator will be a constant that depends only on the total number of samples tested [that is, $N$ in Eq. (11.25)]. The denominator depends on the ratio $\sigma_{\max}/\sigma_{\min}$, which is proportional to the ratio $c_{\min}/c_{\max}$, which is clearly independent of $K_{Ic}$, absent $R$ curve effects. Thus toughening of a solid per se will often not result in an increase in its Weibull modulus. However, it can be easily shown that if a solid exhibits $R$ curve behavior, then an increase in $m$ should, in principle, follow (see Prob. 11.12).

### Effect of size and test geometry on strength

One of the important ramifications of brittle failure, or *weak-link statistics*, as it is sometimes referred to, is the fact that strength becomes a function of volume: *larger specimens will have a higher probability of containing a larger defect, which in turn will cause lower strengths.* In other words, the larger the specimen, the weaker it is likely to be. Clearly, this is an important consideration when data obtained on test specimens, which are usually small, are to be used for the design of larger components.

Implicit in the analysis so far has been that the volumes of all the samples tested were the same size and shape. The probability of a sample of volume $V_0$ surviving a stress $\sigma$ is given by

$$S(V_0) = \exp\left\{-\left[\frac{\sigma}{\sigma_0}\right]^m\right\} \tag{11.27}$$

The probability that a batch of $n$ such samples will all survive the same stress is lower and is given by[205]

$$S_{\text{batch}} = [S(V_0)]^n \tag{11.28}$$

Placing $n$ batches together to create a larger body of volume $V$, where $V = nV_0$, one sees that the probability $S(V)$ of the larger volume surviving a stress $\sigma$ is identical to Eq. (11.28), or

$$S(V) = S_{\text{batch}} = [S(V_0)]^n = [S(V_0)]^{V/V_0} \tag{11.29}$$

which is mathematically equivalent to

$$\boxed{S = \exp\left\{-\left(\frac{V}{V_0}\right)\left(\frac{\sigma}{\sigma_0}\right)^m\right\}} \tag{11.30}$$

This is an important result since it indicates that the survival probability of a ceramic depends on both the volume subjected to the stress and the Weibull modulus. Equation (11.30) states that as the volume increases, the stress level needed to maintain a given survival probability has to be reduced. This can be seen more clearly by equating the survival probabilities of two types of specimens — test specimens with a volume $V_{\text{test}}$ and component specimens with volume $V_{\text{comp}}$. Equating the survival probabilities of the two types of samples and rearranging Eq. (11.30), one can easily show that

$$\frac{\sigma_{\text{comp}}}{\sigma_{\text{test}}} = \left(\frac{V_{\text{test}}}{V_{\text{comp}}}\right)^{1/m} \tag{11.31}$$

A plot of this equation is shown in Fig. 11.22, where the relationship between strength and volume is plotted. The salient point here is that as either the volume *increases* or the Weibull modulus *decreases*, the more severe the downgrading of the design stress required to maintain a given survival probability.

An implicit assumption made in deriving Eq. (11.31) is that only one flaw population (i.e., those due to processing rather than, say, machining) is controlling the strength. Different flaw populations will have different strength distributions and will scale in size differently. Also implicit in deriving Eq. (11.31) is that volume defects are responsible for failure. If, instead, surface flaws were suspected of causing failure, by using a derivation similar to the one used to get to Eq. (11.31), it can be shown that

$$\frac{\sigma_{\text{comp}}}{\sigma_{\text{test}}} = \left(\frac{A_{\text{test}}}{A_{\text{comp}}}\right)^{1/m} \tag{11.32}$$

in which case the strength will scale with area instead of volume.

[205] An analogy here is useful: the probability of rolling a given number with a six-sided die is 1/6. The probability that the same number will appear on $n$ dice rolled simultaneously is $(1/6)^n$.

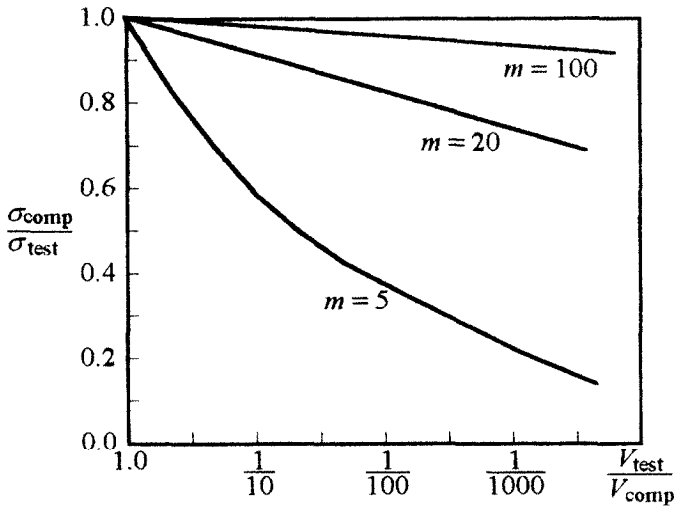


**Figure 11.22** The effect of volume on strength degradation as a function of the Weibull modulus. The strength decreases as $V$ increases and is more severe for low $m$.

Finally, another important ramification of the stochastic nature of brittle fracture is the effect of the stress distribution during testing on the results. When a batch of ceramics is tested in tension, the entire volume and surface are subjected to the stress. Thus a critical flaw *anywhere* in the sample will propagate with equal probability. In three- or four-point flexure tests, however, only one-half the sample is in tension, and the other one-half is in compression. In other words, the effective volume tested is, in essence, reduced. It can be shown that the ratio of the tensile to flexural strength for an equal probability of survival is

$$\frac{\sigma_{\text{3-point bend}}}{\sigma_{\text{tension}}} = [2(m+1)^2]^{1/m} \tag{11.33}$$

In other words, the samples subjected to flexure will appear to be stronger, by a factor that depends on $m$. For example, for $m = 5$, the ratio is about 2, whereas increasing $m$ to 20 reduces the ratio to 1.4.

### 11.5.2 Proof Testing

In proof testing, the components are briefly subjected to a stress level $\sigma_{PT}$ which is in excess of that anticipated in service. The weakest samples fail and are thereby eliminated. The resulting truncated distribution, shown in Fig. 11.20*b*, can be used with a high level of confidence at any stress that is slightly lower than $\sigma_{PT}$.

One danger associated with proof testing is subcritical crack growth, discussed in the next chapter. Since moisture is usually implicated in subcritical crack growth, effective proof testing demands inert, i.e., moisture-free, testing environments and rapid loading/unloading cycles that minimize the time at maximum stress.

## 11.6 Summary

1. Ceramics are brittle because they lack a mechanism to relieve the stress buildup at the tips of notches and flaws. This makes them notch-sensitive, and consequently their strength will depend on the combination of applied stress and flaw size. The condition for failure is

$$K_I = \sigma_f \sqrt{\pi c} \geq K_{Ic}$$

where $K_{Ic}$ is the fracture toughness of the material. The strength of ceramics can be increased by either increasing the fracture toughness or decreasing the flaw size.

2. Processing introduces flaws in the material that are to be avoided if high strengths are to be achieved. The flaws can be pores, large grains in an otherwise fine matrix, and inclusions, among others. Furthermore, since the strength of a ceramic component decreases with increasing grain size, it follows that to obtain a high-strength ceramic, a flaw-free, fine microstructure is desirable.

3. It is possible to toughen ceramics by a variety of techniques, which all make it energetically less favorable for a crack to propagate. This can be accomplished either by having a zone ahead of the crack martensitically transform, thus placing the crack tip in compression, or by adding whiskers or fibers or large grains (duplex microstructures) that bridge the crack faces as it propagates.

   Comparing the requirements for high strength (uniform, fine microstructure) to those needed to improve toughness (nonhomogeneous, duplex microstructure) reveals the problem in achieving both simultaneously.

4. The brittle nature of ceramics together with the stochastic nature of finding flaws of different sizes, shapes, and orientations relative to the applied stress will invariably result in some scatter to their strength. According to the Weibull distribution, the survival probability is given by

$$S = \exp\left\{ -\left(\frac{\sigma}{\sigma_0}\right)^m \right\}$$

where $m$, known as the *Weibull modulus*, is a measure of the scatter. Large scatter is associated with low $m$ values, and vice versa.

5. If strength is controlled by defects randomly distributed within the volume, then strength becomes a function of volume, with the survival probability decreasing with increasing volume. However, if strength is controlled by surface defects, strength will scale with area instead.

6. Proof testing, in which a component is loaded to a stress level higher than the service stress, eliminates the weak samples, truncating the distribution and establishing a well-defined stress level for design.

## Problems

**11.1.** (*a*) Following a similar analysis used to arrive at Eq. (11.7), show that an internal crack of length $c$ is only $\sqrt{2}$ as detrimental to the strength of a ceramic as a surface crack of the same length.

(*b*) Why are ceramics usually much stronger in compression than in tension?

(*c*) Explain why the yield point of ceramics can approach the ideal strength $\sigma_{\text{theo}}$, whereas the yield point in metals is usually much less than $\sigma_{\text{theo}}$. How would you attempt to measure the yield strength of a ceramic, given that the fracture strength of ceramics in tension is usually much less than the yield strength?

**11.2.** (*a*) Estimate the size of the critical flaw for a glass that failed at 102 MPa if $\gamma = 1\,\text{J m}^2$ and $Y = 70\,\text{GPa}$.

*Answer*: 4.3 μm

(*b*) What is the maximum stress this glass will withstand if the largest crack is on the order of 100 μm and the smallest on the order of 7 μm?

*Answer*: 21 MPa

**11.3.** Show that Eqs. (11.2) and (11.9) are equivalent, provided the radius of curvature of the crack $\rho \approx 14r_0$, where $r_0$ is the equilibrium interatomic distance; in other words, if it is assumed that the crack is atomically sharp. *Hint*: Find expressions for $\gamma$ and $Y$ in terms of $n$, $m$, and $r_0$ defined in Chap. 4. You can assume $n = 9$ and $m = 1$.

**11.4.** $Al_2O_3$ has a fracture toughness $K_{Ic}$ of about $4\,\text{MPa} \cdot \text{m}^{1/2}$. A batch of $Al_2O_3$ samples were found to contain surface flaws about 30 μm deep. The average flaw size was more on the order of 10 μm. Estimate (*a*) the tensile strength and (*b*) the compressive strength.

*Answer*: 412 MPa, 10 GPa

**11.5.** To investigate the effect of pore size on the strength of reaction-bonded silicon nitride, Heinrich[206] introduced artificial pores (wax spheres that melt during processing) in his compacts prior to reaction bonding. The results he obtained are summarized below. Are these data consistent with the Griffith criterion? Explain clearly, stating all assumptions.

[206] J. Heinrich, *Ber. Dt. Keram. Ges.*, **55** (1978).

| Wax grain size, μm | Average pore size, μm | Bend strength, MPa |
|---|---|---|
| 0–36 | 48 | 140 ± 12 |
| 63–90 | 66 | 119 ± 12 |
| 125–180 | 100 | 101 ± 14 |

**11.6.** The tensile fracture strengths of three different structural ceramics are listed below: hot-pressed silicon nitride (HPSN), reaction-bonded silicon nitride (RBSN), and chemical vapor-deposited silicon carbide (CVDSC), measured at room temperature.

(*a*) Plot the cumulative *failure probability* of these materials as a function of fracture strength.

(*b*) Calculate the mean strength and standard deviation of the strength distributions, and determine the Weibull modulus for each material.

(*c*) Estimate the design stress for each material.

(*d*) On the basis of your knowledge of these materials, why do you think they behave so differently?

| | |
|---|---|
| HPSN (MPa) | 521, 505, 500, 490, 478, 474,471,453, 452, 448, 444, 441, 439, 430, 428, 422, 409, 398, 394, 372, 360,341, 279 |
| CVDSC | 386, 351, 332, 327, 308, 296, 290, 279, 269, 260, 248, 231, 219, 199, 178, 139 |
| RBSN | 132, 120, 108, 106, 103, 99, 97, 95, 93, 90, 89, 84, 83, 82, 80, 80, 78, 76 |

**11.7.** (*a*) When the ceramic shown in Fig. 11.23 was loaded in tension (along the length of the sample), it fractured at 20 MPa. The

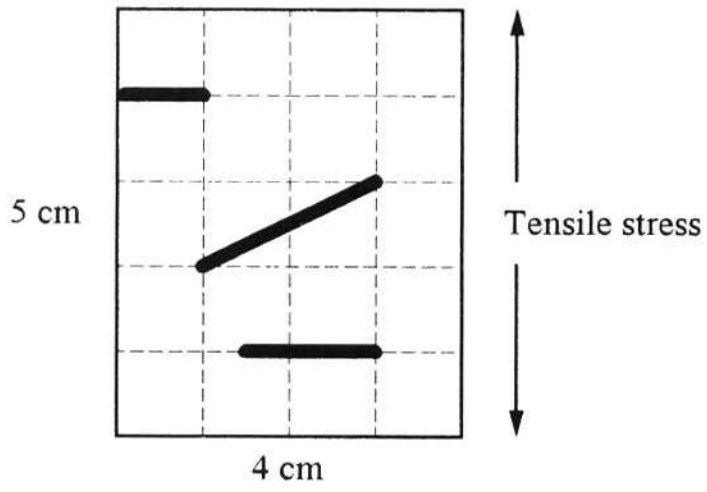


**Figure 11.23** Cross section of ceramic part loaded in tension as shown. The heavy lines denote flaws.

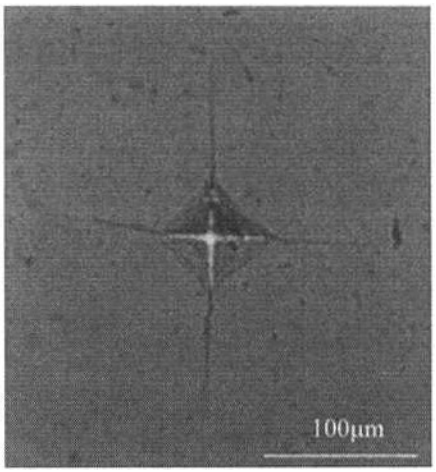


**Figure 11.24** Optical photomicrograph of indentation in glass. 200×.

heavy lines denote cracks (two internal and one surface crack). Estimate $K_{Ic}$ for this ceramic. State all assumptions.

*Answer*: 3.5 MPa · $m^{1/2}$

**11.8.** For silicon nitride, $K_{Ic}$ is strongly dependent on microstructure, but can vary anywhere from 3 to 10 MPa · $m^{1/2}$. Which of the following silicon nitrides would you choose, one in which the largest flaw size is on the order of 50 μm and the fracture toughness is 8 MPa · $m^{1/2}$, or one for which the largest flaw size was 25 μm, but was only half as tough. Explain.

**11.9.** Evans and Charles[207] proposed the following equation for the determination of fracture toughness from indentation:

$$K_{Ic} \approx 0.15(H\sqrt{a})\left(\frac{c}{a}\right)^{-1.5}$$

where $H$ is the Vickers hardness in Pa and $c$ and $a$ were defined in Fig. 11.7. A photomicrograph of a Vickers indention in a glass slide and the cracks that emanate from it is shown in Fig. 11.24. Estimate the fracture toughness of this glass if its hardness is ≈5.5 GPa.

*Answer*: ≈1.2 to 1.6 MPa · $m^{1/2}$ depending on size of crack calculated

**11.10.** A manufacturer wishes to choose between two ceramics for a certain application. Data for the two ceramics tested under identical conditions were as follows:

| Ceramic | Mean fracture stress | Weibull modulus |
|---|---|---|
| A | 500 MPa | 12 |
| B | 600 MPa | 8 |

[207] A. G. Evans and E. A. Charles, *J. Amer. Cer. Soc.*, **59**:317 (1976).

The service conditions are geometrically identical to the test conditions and impose a stress of 300 MPa. By constructing Weibull graphs with $S = 1/2$ for mean fracture stress or any other method, decide which ceramic will be more reliable and compare the probabilities of failure at 300 MPa. At what stress would the two ceramics give equal performance?

*Answer*: Stress for equal performance = 349 MPa

**11.11.** The MORs of a series of cylindrical samples ($l = 25$ mm and diameter of 5 mm) were tested and analyzed using Weibull statistics. The average strength was 100 MPa, with a Weibull modulus of 10. Estimate the stress required to obtain a survival probability of 95 percent for cylinders with diameters of 10 mm but the same length. State all assumptions.

**11.12.** Show why ceramics that exhibit $R$ curve behavior should, in principle, also exhibit larger $m$ values.

**11.13.** (*a*) In deriving Eq. (11.30) the flaw population was assumed to be identical in both volumes. However, sometimes in the manufacturing of ceramic bodies of different volumes and shapes, different flaw populations are introduced. What implications, if any, does this statement have on designing with ceramics? Be specific.

(*b*) In an attempt to address this problem, Kschinka *et al.*[208] measured the strength of different glass spheres in compression. Their results are summarized in Table 11.3, where $D_0$ is the diameter of the glass spheres, $N$ is the number of samples tested, $m$ is the Weibull modulus, $\sigma_f$ is the average strength, and $V$ is the volume of the spheres.

**Table 11.3**

| $D_0$, cm | $N$ | $m$ | $\sigma_f$ (50%) | $V$, cm$^3$ |
|---|---|---|---|---|
| 0.368 | 47 | 6.19 | 143 | $2.61 \times 10^{-2}$ |
| 0.305 | 48 | 5.96 | 157 | $1.49 \times 10^{-2}$ |
| 0.241 | 53 | 5.34 | 195 | $7.33 \times 10^{-3}$ |
| 0.156 | 30 | 5.46 | 229 | $1.99 \times 10^{-3}$ |
| 0.127 | 45 | 5.37 | 252 | $1.07 \times 10^{-3}$ |
| 0.108 | 38 | 5.18 | 303 | $6.60 \times 10^{-4}$ |
| 0.091 | 47 | 3.72 | 407 | $3.95 \times 10^{-4}$ |
| 0.065 | 52 | 4.29 | 418 | $1.44 \times 10^{-4}$ |
| 0.051 | 44 | 6.82 | 435 | $6.95 \times 10^{-5}$ |

[208] B. A. Kschinka, S. Perrella, H. Nguyen, and R. C. Bradt, *J. Amer. Cer. Soc.*, **69**:467 (1986).

(i) Draw on *one graph* the Weibull plots for spheres of 0.051, 0.108, and 0.368 cm. Why are they different?
(ii) For the 0.051 cm spheres, what would be your design stress to ensure a 0.99 survival probability?
(iii) Estimate the average strength of glass spheres of 1-cm diameter.
(iv) If the effect of volume is taken into account, then it is possible to collapse all the data on a master curve. Show how that can be done. *Hint*: Normalize data to 0.156-cm spheres, for example.

## Additional Reading

1. R. W. Davidge, *Mechanical Behavior of Ceramics*, Cambridge University Press, New York, 1979.
2. R. Warren, ed., *Ceramic Matrix Composites*, Blackie, Glasgow, Scotland, 1992.
3. B. Lawn, *Fracture of Brittle Solids*, 2d ed., Cambridge University Press, New York, 1993.
4. A. Kelly and N. H. Macmillan, *Strong Solids*, 3d ed., Clarendon Press, Oxford, England, 1986.
5. G. Weaver, "Engineering with Ceramics, Parts 1 and 2," *J. Mat. Ed.*, **5**:767 (1983) and **6**:1027 (1984).
6. T. H. Courtney, *Mechanical Behavior of Materials*, McGraw-Hill, New York, 1990.
7. A. G. Evans, "Engineering Property Requirements for High Performance Ceramics," *Mat. Sci. & Eng.*, **71**:3 (1985).
8. S. M. Weiderhorn, "A Probabilistic Framework for Structural Design," in *Fracture Mechanics of Ceramics*, vol. 5, R. C. Bradt, A. G. Evans, D. P. Hasselman, and F. F. Lange, eds., Plenum, New York, 1978, p. 613.
9. M. F. Ashby and B. F. Dyson, in *Advances in Fracture Research*, S. R. Valluri, D. M. R. Taplin, P. Rama Rao, J. F. Knott, and R. Dubey, eds., Pergamon Press, New York, 1984, p. 3.
10. P. F. Becher, "Microstructural Design of Toughened Ceramics," *J. Amer. Cer. Soc.*, **74**:225 (1991).